Journal of Advanced Research 10 (2018) 49–67

Contents lists available at ScienceDirect

Journal of Advanced Research

journal homepage: www.elsevier.com/locate/jare

Review

Strengthening mechanisms, deformation behavior, and anisotropic mechanical properties of Al-Li alloys: A review

Ali Abd El-Aty [a,b,1], Yong Xu [a,1,*], Xunzhong Guo [c], Shi-Hong Zhang [a], Yan Ma [a], Dayong Chen [a]

[a] Institute of Metal Research, Chinese Academy of Sciences, Shenyang 110016, PR China
[b] School of Engineering Science, University of Chinese Academy of Sciences, Beijing 100049, PR China
[c] College of Material Science and Technology, Nanjing University of Aeronautics and Astronautics, Nanjing 211100, PR China

GRAPHICAL ABSTRACT

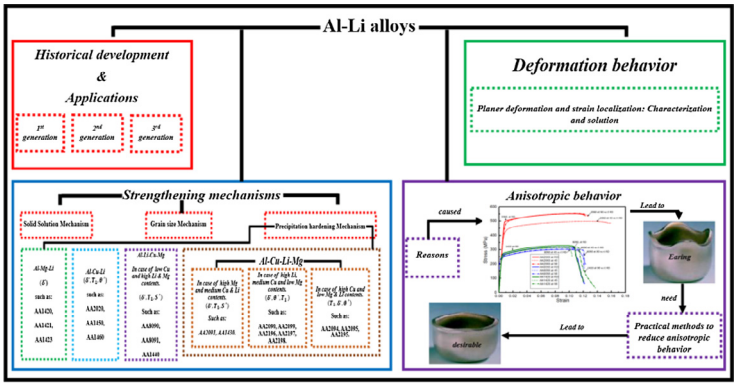

ARTICLE INFO

Article history:
Received 11 September 2017
Revised 7 December 2017
Accepted 23 December 2017
Available online 26 December 2017

Keywords:
Al-Li alloys
Anisotropic behavior
Strengthening
Deformation mechanism
Formability

ABSTRACT

Al-Li alloys are attractive for military and aerospace applications because their properties are superior to those of conventional Al alloys. Their exceptional properties are attributed to the addition of Li into the Al matrix, and the technical reasons for adding Li to the Al matrix are presented. The developmental history and applications of Al-Li alloys over the last few years are reviewed. The main issue of Al-Li alloys is anisotropic behavior, and the main reasons for the anisotropic tensile properties and practical methods to reduce it are also introduced. Additionally, the strengthening mechanisms and deformation behavior of Al-Li alloys are surveyed with reference to the composition, processing, and microstructure interactions. Additionally, the methods for improving the formability, strength, and fracture toughness of Al-Li alloys are investigated. These practical methods have significantly reduced the anisotropic tensile properties and improved the formability, strength, and fracture toughness of Al-Li alloys. However, additional endeavours are required to further enhance the crystallographic texture, control the anisotropic behavior, and improve the formability and damage tolerance of Al-Li alloys.

Introduction

Recently, Al-Li alloys have gained attention for their use in weight and stiffness-critical structures used in aircraft, aerospace and military applications because they exhibit better properties,

Peer review under responsibility of Cairo University.
* Corresponding author.
E-mail address: yxu@imr.ac.cn (Y. Xu).
[1] These authors equally contributed to this study.

https://doi.org/10.1016/j.jare.2017.12.004
2090-1232/

such as a low density and high specific strength, than those of commercial Al alloys [1–4]. The Improvements in density and specific strength are not only the factors of measuring the performance for aerospace materials. Damage tolerance (e.g., fatigue crack growth and residual strength) and durability (e.g., fatigue and corrosion resistance) properties generally control the dimensions of the aircraft and aerospace components. The engineering properties of most significance are a function of the aircraft components such as empennage, fuselage, lower or upper or wing and position on the aircraft. Fig. 1 depicts the engineering properties required for different structural areas in transport aircraft [5]. These engineering properties vary for various areas, but definitely, there are many commonalities.

The superior properties of the Al-Li alloys are mainly attributed to the added Li, which influences the weight reduction and elastic modulus. As previously reported, 1 wt% of Li decreases the density of the resultant Al alloy by approximately 3% and increases the elastic modulus by approximately 6%, as depicted in Fig. 2a and b, respectively [4,6,7]. Since Al is a lightweight metal (2.7 g/cm^3), few alloying addition choices exist for a further weight reduction. Si (2.33 g/cm^3), Be (1.848 g/cm^3), Mg (1.738 g/cm^3), and Li (0.534 g/cm^3) are the only elementary metallic metals with a lower density than Al that can be alloyed with Al. Li is the lightest metal and least dense solid element of these metals, and only Mg and Li possess moderate solubilities in the Al matrix. Adding Mg to Al results in alloys with poor stiffness and low corrosion properties [8–10]. However, adding Li to Al improves the solubility of Al at high temperatures and produces fine precipitates, which improve the stiffness and strength of the Al alloys [11]. Because of these aspects, Li is the optimum metallic element for Al alloys. Compared with traditional Al alloys, Al-Li alloys exhibit better stiffness, strength, and fracture toughness and a lower density [12–14]. Additionally, the fracture toughness of Al-Li alloys at cryogenic temperatures is higher than that of traditional Al alloys. Al-Li alloys also have higher resistance to fatigue crack growth and stress corrosion cracking than traditional Al alloys [15–17].

Unfortunately, in addition to the benefits obtained by adding Li to Al, decreases in the ductility, formability, and fracture toughness as well as anisotropic mechanical properties are also obtained in Al-Li alloys. These shortcomings resulted in previous Al-Li alloy grades inappropriate for a variety of commercial applications [4].

The development of rapid solidification technology (RST), i.e., rapid solidification or rapid quenching, is key for enhancing the mechanical properties of Al-Li alloys [18]. RST has advantages over ingot metallurgy methods for the production of Al-Li alloys [4]. The advantages include (a) the combination of more Li with the highest value of 2.7 wt% for the ingot alloys; (b) the use of strengthening mechanisms, such as substructure and precipitation hardening; (c) the enhancement of the quantity (wt%) of the alloying components; and (d) the refinement of the second phases [3,4,18]. While the mechanical properties of Al-Li alloys have been improved by RST, various issues, such as their poor formability and fracture behavior, still persist and are barriers to further improvements in Al-Li alloys. Methods such as numerous alloy chemistry adaptations and novel thermomechanical processing (TMP) techniques have been used to reduce anisotropic mechanical properties as well as enhance the formability and fracture toughness of Al-Li alloys while maintaining their high specific stiffness and strength [3,18].

While large increases in the fracture toughness, ductility, formability, and other properties have been obtained using RST and TMP, a few disadvantages remain. Besides, the cost of Al-Li alloys is higher than that of traditional Al alloys because of the ageing conditions and comparable strength. Therefore, various studies have been carried out to investigate metal forming technologies (i.e., hydroforming, impact hydroforming, stamping, bending, and superplastic forming) under different working conditions (i.e., cold, warm, and hot deformation) to identify an alternative manufacturing route and to optimize the working conditions to decrease the higher costs related to the addition of Li and the manufacturing of sound, complex shape components from Al-Li alloys [19–49].

A review of the current literature on novel Al-Li alloys is extraordinarily valuable for understanding the different techniques that have been used to improve the mechanical properties and formability, and to provide context for future investigations. The serious issues concerning the metallurgical aspects that affect the micro-mechanisms controlling the strengthening, deformation, and fracture behavior are explained to further the understanding of the key failure mechanisms. In addition, the texture and anisotropy behavior of Al-Li alloys and possible methods to address these issues are also discussed. Current research results are noted, and some successful, previous investigations are also included. We hope that this comprehensive review will offer an explanation of the mechanical behavior and relevant anisotropy, deformation and strengthening of Al-Li alloys and the key methods that will lead to success with the third generation of Al-Li alloys. We start

Fig. 1. Engineering properties needed for transport aircraft, where: FAT = Fatigue; FT = Fracture Toughness; FCG = Fatigue Crack Growth (FAT, FT and FCG are denoted as Damage Tolerance (DT)); E = Elastic Modulus; TS = Tensile Strength; SS = Shear Strength; CYS = Compressive Yield Strength; ( ) = Important, but not critical property. [5]

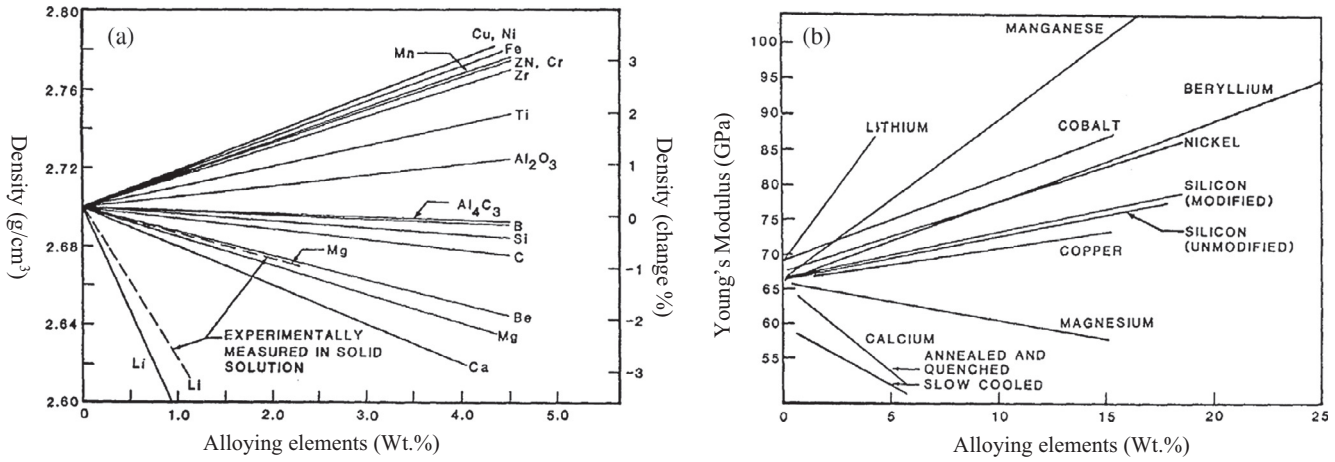

Fig. 2. Effect of alloying elements on the (a) density; and (b) elastic modulus of Al Alloys [4].

with a brief discussion of the historical developments and applications of Al-Li alloys.

History of the development of Al-Li alloys and their applications

First (1st) generation Al-Li alloys and their applications

In the 1950s, researchers at the Alcoa Company observed that Li improved the elastic modulus (stiffness) of Al, and they obtained U. S. patents for their discoveries [50–52]. In 1957, the high-strength Al-Cu-Li alloy 2020 was developed by the Alcoa Company (see Table 1), and this alloy possessed a high strength and high creep resistance in the temperature range of 150–200 °C. The 2020 alloy was commercially produced and used to manufacture the wings of the United States Navy's RA-5C Vigilante aircraft for more than 20 years without a single documented fracture (crack or corrosion issues) [3,8].

In the 1960s, the 2020 alloy was withdrawn from commercial applications because of manufacturing issues, which were attributed to its high brittleness and poor ductility. The 2020 alloy ductility issue is attributed to the high wt% of Si and Fe used for advanced aircraft alloys. During the solidification and successive processing, these particles precipitate as the insoluble component phases, Al_{12}-$(FeMn)_3Si$ and Al_7Cu_2Fe, and change in size from 1 to 10 μm [53–59]. During working operations, these large particles begin to crack and cause a non-uniform strain distribution, which improves the probability of recrystallization during successive heat treatments [59].

In the early 1960s, further work in the former Soviet Union resulted in an improvement of plates from the alloy VAD23, which is similar to the 2020 alloy, and improvements in the sheet, plate,

Table 1
Densities, developers and chemical compositions of key Al-Li alloys developed to-date (adopted from Rioja et al. [3]).

Alloy	Li wt%	Cu wt%	Mg wt%	Ag wt%	Zr wt%	Sc wt%	Mn wt%	Zn wt%	Al wt%	Density ρ (g/cm³)	Place, Data
First generation											
2020	1.2	4.5					0.5		Balance	2.71	Alcoa, 1958
1420	2.1		5.2		0.11					2.47	Soviet, 1965
1421	2.1		5.2		0.11	0.17				2.47	Soviet, 1965
Second generation (Li ⩾ 2 wt%)											
2090	2.1	2.7			0.11				Balance	2.59	Alcoa, 1984
2091	2.0	2.0	1.3		0.11					2.58	Pechiney, 1985
8090	2.4	1.2	0.8		0.11					2.54	EAA, 1984
1430	1.7	1.6	2.7		0.11	0.17				2.57	Soviet, 1980s
1440	2.4	1.5	0.8		0.11					2.55	Soviet, 1980s
1441	1.95	1.65	0.9		0.11					2.59	Soviet, 1980s
1450	2.1	2.9			0.11					2.60	Soviet, 1980s
1460	2.25	2.9			0.11					2.60	Soviet, 1980s
Third generation (Li < 2 wt%)											
2195	1.0	4.0	0.4	0.4	0.11				Balance	2.71	LM/Reynolds, 1992
2196	1.75	2.9	0.5	0.4	0.11		0.35 max	0.35 max		2.63	LM/Reynolds, 2000
2297	1.4	2.8	0.25 max		0.11		0.3	0.5 max		2.65	LM/Reynolds, 1997
2397	1.4	2.8	0.25 max		0.11		0.3	0.10		2.65	Alcoa, 2002
2098	1.05	3.5	0.53	0.43	0.11		0.35 max	0.35		2.70	McCook- Metals, 2000
2198	1.0	3.2	0.5	0.4	0.11		0.5 max	0.35 max		2.69	Reynolds/ McCook- Metals/Alcan, 2005
2099	1.8	2.7	0.3		0.09		0.3	0.7		2.63	Alcoa, 2003
2199	1.6	2.6	0.2		0.09		0.3	0.6		2.64	Alcoa, 2005
2050	1.0	3.6	0.4	0.4	0.11		0.35	0.25 max		2.70	Pechiney/ Alcan 2004
2296	1.6	2.45	0.6	0.43	0.11		0.28	0.25 max		2.63	Alcan, 2010
2060	0.75	3.95	0.85	0.25	0.11		0.3	0.4		2.72	Alcoa, 2011
2055	1.15	3.7	0.4	0.4	0.11		0.3	0.5		2.70	Alcoa, 2012
2065	1.2	4.2	0.5	0.30	0.11		0.4	0.2		2.70	Constellium, 2012
2076	1.5	2.35	0.5	0.28	0.11		0.33	0.30 max		2.64	Constellium, 2012

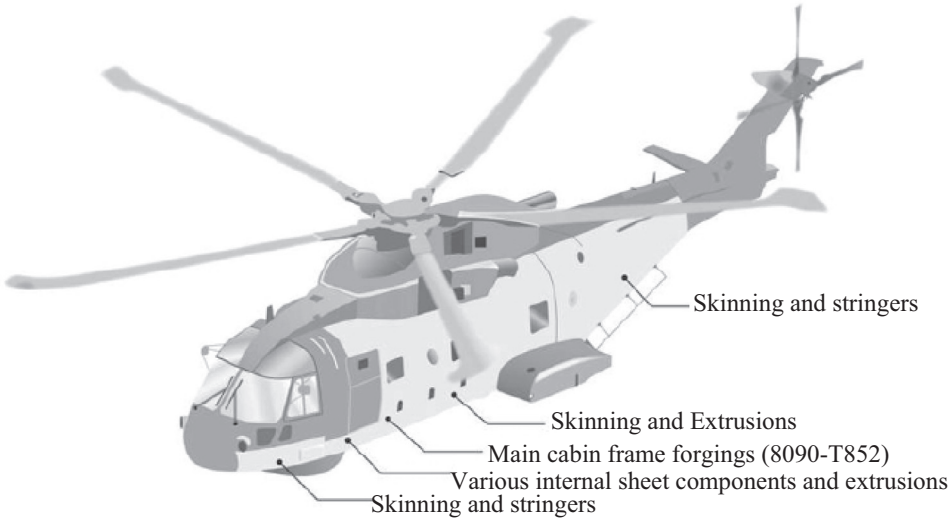

Fig. 3. Use of alloy AA8090 on the Agusta-Westland EH101 [5]

forgings and extrusions from alloys 1420 and 1421, which were successfully used in Soviet Union aircraft [52–57]. Alloy 1420 has one of the lowest densities available for a commercial alloy [58,59]. For this alloy, the improvement in the weldability and the solid solution strengthening obtained from adding 5.2 wt% Mg were combined with the advantages obtained by adding 2 wt % Li. Moreover, 0.11 wt% Zr was added to govern the grain growth and recrystallization. In 1971, the vertical take-off and landing aircrafts, Âk36 and Âk38, were produced using alloy 1420. In the 1980s, the Soviet Union possessed plans to manufacture hundreds of Al-Li MiG29s by welding; however, after the cold war with the United States was resolved, the manufacturing ceased [54,59]. Although alloy 1420 offers a low density and a good weldability and stiffness, its strength and fracture toughness are not sufficient to meet the requirements of modern aircraft. The main reason for the poor fracture toughness is due to shearing of Al_3Li (main strengthening phase), which causes planar slip. Therefore, further investigations have examined different compositions to determine other non-shearable phases that can decrease the planar slip tendency and cause additional alloy hardening [55–59]. The densities, developers and nominal compositions of key Al-Li alloys that have been commercially produced are summarized in Table 1.

Second (2nd) generation Al-Li alloys and their applications

As a result of the previously mentioned issues, 2nd generation Al-Li alloys were created with the objective of obtaining alloys that are lighter (8–10%) and stiffer than traditional Al alloys for aerospace and aircraft applications [59]. Accordingly, in the 1970s and 1980s, various researchers concentrated on reducing the Si and Fe contents to the lowest amounts required for a high ductility and toughness. Mn was replaced with Zr to produce Al_3Zr precipitates for grain refinement, which have an excellent effect on the nucleating voids, ductility and toughness. For nucleating strengthening precipitates, Cd was not used because it was unable to improve the intergranular fracture of alloy 2020 [59,60]. This research contributed to the improvements in the 2nd generation of Al-Li alloys. The Alcoa Company successfully replaced alloy 7075-T6 with 2nd generation Al-Li products, such as 2090-T86 extrusions, 2090-T83 and T84 sheets and 2090-T81 plate. The Pechiney Company replaced the alloy 2024-T3 sheet with 2091-T8X, and British Aerospace replaced the alloy 2024-T3 plate with the 8090-T81 plate [3,61,62]. In the late 1980s, the former Soviet Union improved the 2nd generation of Al-Li alloys by their own methods. They unveiled the specialized benefits of 01450 and 01460 (as 2090), 01440 (as 8090), and 01430 (as 2091) wrought products [61–64].

While the density reduction is appealing, 2nd generation Al-Li alloys had a few characteristics that were viewed as undesirable by airframe designers and manufacturers. Therefore, the applications of 2nd generation Al-Li alloys were restricted, i.e., to aircraft structures. For example, alloy 2090 was used in C-17 cargo transport, alloys 2090 and 8090 were used in A340, and alloy 8090 was used in the EH101 helicopter, as shown in Fig. 3 [5]. The main advantages and disadvantages of 2nd generation Al-Li alloys are summarized in Table 2 [3].

Third (3rd) generation Al-Li alloys and their applications

In the early 1990s, 3rd generation Al-Li alloys were introduced to the market, and these alloys featured a reduced Li concentration (Li < 2 wt%) to overcome the previously mentioned limitations of former Al-Li alloys [3,8,65]. Alloys such as AA2076, AA2065, AA2055, AA2060, AA2050, AA2199, AA2099, AA2397, AA2297, AA2198, AA2196, and AA2195 were developed for aircraft and aerospace applications, and they are 3rd generation Al-Li alloys [65]. The densities, developers, and nominal compositions of 3rd generation Al-Li alloys are listed in Table 1.

The mechanical and physical properties of the 3rd generation Al-Li alloys were tailored to fulfil the requirements of the future aircraft, including weight savings, reduced inspection and maintenance, and performance [3]. For instance, Al-Li alloy 2195 was used instead of AA2219 for the cryogenic fuel tank on the space shuttle, because it provides a lower density, higher modulus and

Table 2
Advantages and disadvantages of 2nd generation Al-Li alloys.

2nd generation Al-Li Alloys (Li ⩾ 2 wt%) and (Cu < 3 wt%)	
Advantages	Disadvantages
Lower Density (from 7% to 10%)	Low short-transverse properties and plane stress (Kc) fracture toughness
High modulus of elasticity (from 10% to 15%)	High anisotropy of mechanical properties
Lower fatigue crack growth rates	Delamination issues during manufacturing

strength than the AA2219. Al-Li alloy 2198-T851 was produced to substitute the AA2524-T3 and AA2024 in aircraft structures, because it has an excellent damage tolerance, low density, and high fatigue resistance compared with the stated alloys [8].

Al-Li alloy 2099 extrusions, plates, and forgings can be used instead of 7xxx, 6xxx, and 2xxx Al alloys in their applications, such as dynamically and statically loaded fuselage structures and lower wing stringers. This might be due to their superior properties compared to the aforementioned Al alloys. As shown in Fig. 4, Al-Li alloy 2099-T83 extrusions has replaced AA7050-T7451 for internal fuselage structures, since it possesses high stiffness, low density, excellent weldability and corrosion resistance, and superior damage tolerance. Additionally, Al-Li alloy 2099 plates and forgings can replace AA7050- T74 and AA7075-T73 Al alloys, because they have low density, high modulus, good strength, and excellent corrosion resistance.

Al-Li alloys 2199-T8E79 plates and 2199-T8 sheets are used in the aircraft rather than (AA2024-T351, AA2324-T39, AA2624-T351, and AA2624-T39) and (AA2024-T3, AA2524-T3, and AA2524-T351) to lower wing stringers and fuselage skin, respectively (Fig. 4). This was attributed to their superior mechanical and physical properties compared with other alloys [8,65].

Al-Li alloy 2050 was introduced to replace 7xxx and 2xxx in the applications, which required high damage tolerance as well as medium to high strength. Al-Li alloy 2050-T84 replaced AA2024-T351, AA7150-T7751, and AA7050-T7451 for lower wing cover, upper wing cover, and rips and other internal structures, respectively, as presented in Fig. 4 [5,8].

Al-Li alloys 2055 and 2060 are the newest 3rd generation Al-Li alloys launched by Alcao Inc. at 2012 and 2011, respectively [1,8]. These alloys replaced AA2024-T3 and AA7075-T6 for fuselage, upper and lower wings structures, as shown in Fig. 4. This is because they exhibit excellent corrosion resistance, high thermal stability, and a synergy of high strength and good toughness. It was reported that replacing 2055-T8 alloy with 7055-T7751 may save 10% weight. Additionally, using 2060-T8 for fuselage skin and lower wing structures instead of AA2524-T3 and 2024-T351 may save 7% and 14%, respectively [8,65]. Table 3 summarizes the key alloys of 3rd generation Al-Li alloy used to replace the traditional Al alloys.

Strengthening mechanisms of Al-Li alloys

The solution of Li element in Al matrix makes only a small degree of the solid solution strengthening, which is mainly created by the variation of the elastic modulus and size of the Li and Al atoms [66]. On the other hand, the main strengthening in Al-Li alloys is generally achieved from the existence of a huge volume fraction of the Al_3Li (δ') phase, which is the main reason for high elastic modulus observed in these alloys, since Al_3Li itself has a large intrinsic modulus [2,3,9,66]. Strengthening by Al_3Li is caused by several mechanisms such as coherency and surface hardening, modulus hardening and order hardening [67]. The effect of modulus hardening and order hardening on improving the strength of Al-Li alloys is higher than the effect of coherency and surface hardening due to the creation of APBs (antiphase boundaries) [68]. The influence of these mechanisms on the strength in terms of shear stress for the slip to happen is presented in Fig. 5a [68]. In order to reduce the energy needed to create the APB, the dislocations in Al–Li alloys flow in pairs combined with a range of APB, such that flow of the second dislocation improves the clutter created by the first dislocation [66]. The critical resolved shear stress for such a process is described by Eq. (1) as follows:

$$\tau_{CRSS} \propto (\gamma^{APB})^{\frac{3}{2}} \cdot r^{\frac{1}{2}} \cdot f^{1/2} \quad (1)$$

where τ_{CRSS} is acritical resolved shear stress, γ is APB energy of Al_3Li particles, r is the mean radius of the particles, and f is the volume fraction of the particles. After shearing, the ordered precipitates may lead to reducing the contributions from order strengthening, which is necessary because of the reduction in the cross section area of the precipitates at the beginning of shearing [66–68]. For n_d dislocations, let's suppose that each dislocation has a Burger's vector b_v, and the shearing occurred at the diameter of the precipitates, in order to shear a certain precipitate or particle, the required τ_{CRSS} stress is:

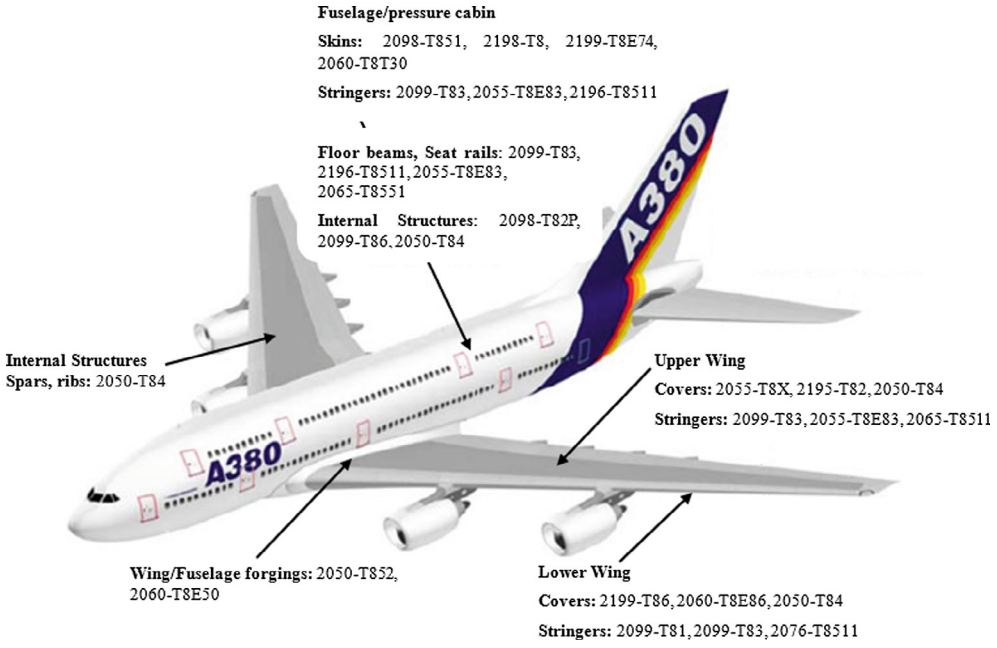

Fig. 4. Actual and proposed used of 3rd generation Al-Li alloys in a transport aircraft (adopted from Wanhill et al. [5]).

Table 3
Actual and proposed uses of 3rd generation Al-Li alloys to replace Traditional Al alloys aircrafts (adopted from Wanhill et al. [5]).

Product	Al-Li Alloy	Required engineering property	Substitute for	Applications
Sheet	2098-T851, 2198-T8, 2199-T8E74, 2060-T8E30	Damage tolerant/ medium strength	2024-T3, 2524-T3, 2524-T351	Fuselage/pressure cabin skins
Plate	2199-T86, 2050-T84, 2060-T8E86	Damage tolerant	2024-T351, 2324-T39, 2624-T351, 2624-T39	Lower wing covers
	2098-T82P (sheet/plate)	Medium strength	2024-T62	F-16 fuselage panels
	2297-T87, 2397-T87	Medium strength	2124-T851	F-16 fuselage bulkheads
	2099-T86	Medium strength	7050-T7451, 7X75-T7XXX	Internal fuselage structures
	2050-T84, 2055-T8X, 2195-T82	High strength	7150-T7751, 7055- T7751, 7055-T7951, 7255-T7951	Upper wing covers
	2050-T84	Medium strength	7050-T7451	Spars, ribs, other internal structures
	2195-T82/T84	High strength	2219-T87	Launch vehicle cryogenic tanks
Forgings	2050-T852, 2060-T8E50	High strength	7175-T7351, 7050-T7452	Wing/fuselage attachments, window and crown frames
Extrusions	2099-T81, 2076-T8511	Damage tolerant	2024-T3511, 2026-T3511, 2024-T4312, 6110-T6511	Lower wing stringers Fuselage/pressure cabin stringers
	2099-T83, 2099-T81, 2196-T8511, 2055-T8E83, 2065-T8511	Medium/high strength	7075-T73511, 7075-T79511, 7150-T6511, 7175-T79511, 7055-T77511, 7055-T79511	Fuselage/pressure cabin stringers and frames, upper wing stringers, Airbus A380 floor beams and seat rails

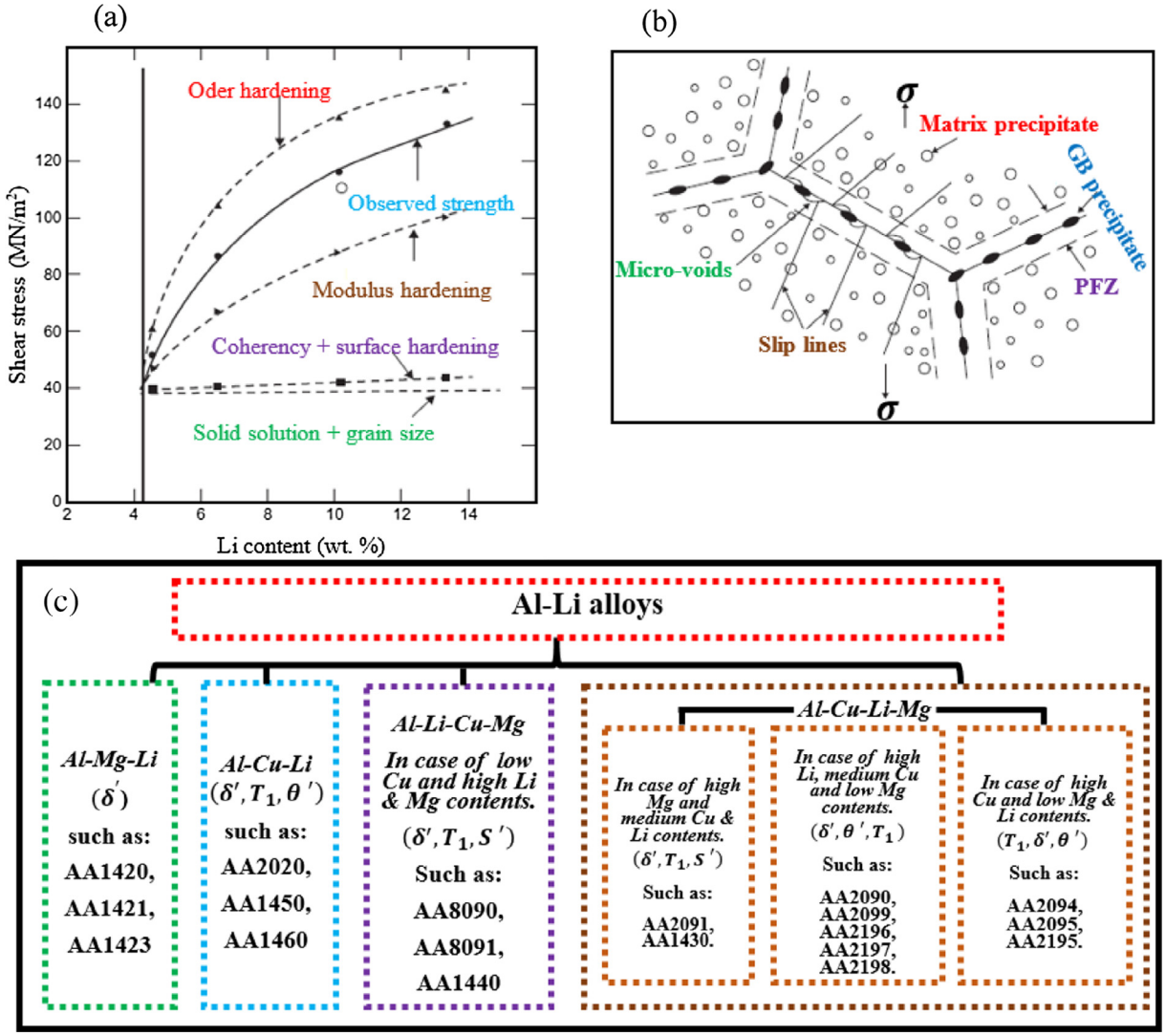

Fig. 5. Schematic representation of (a) contribution of different strengthening mechanisms by Al_3Li [66]; (b) void nucleation at GB particles when PEZs are exist [66]; (c) strengthening phases in (Al-Li-Cu) and (Al-Li-Cu-Mg) alloys; (d) a simplified explanation of precipitates microstructural in 2nd. and (e) 3rd generation Al-Li alloys [68]; (f) a graphical representation of structure of complex precipitates which constitute in Al-Li-X alloys [59], where: δ′ = (Al_3Li); δ = (AlLi) equilibrium phase; θ′ = (Al_2Cu); β′ = (Al_3Zr); T1 = (Al_2CuLi) equilibrium phase; T2 = (Al_6CuLi_3) equilibrium phase; S′ = (Al_2CuMg), M = Major relative volume fraction and S = Minor relative volume fraction. The phases mentioned are found in different conditions of heat treatment.

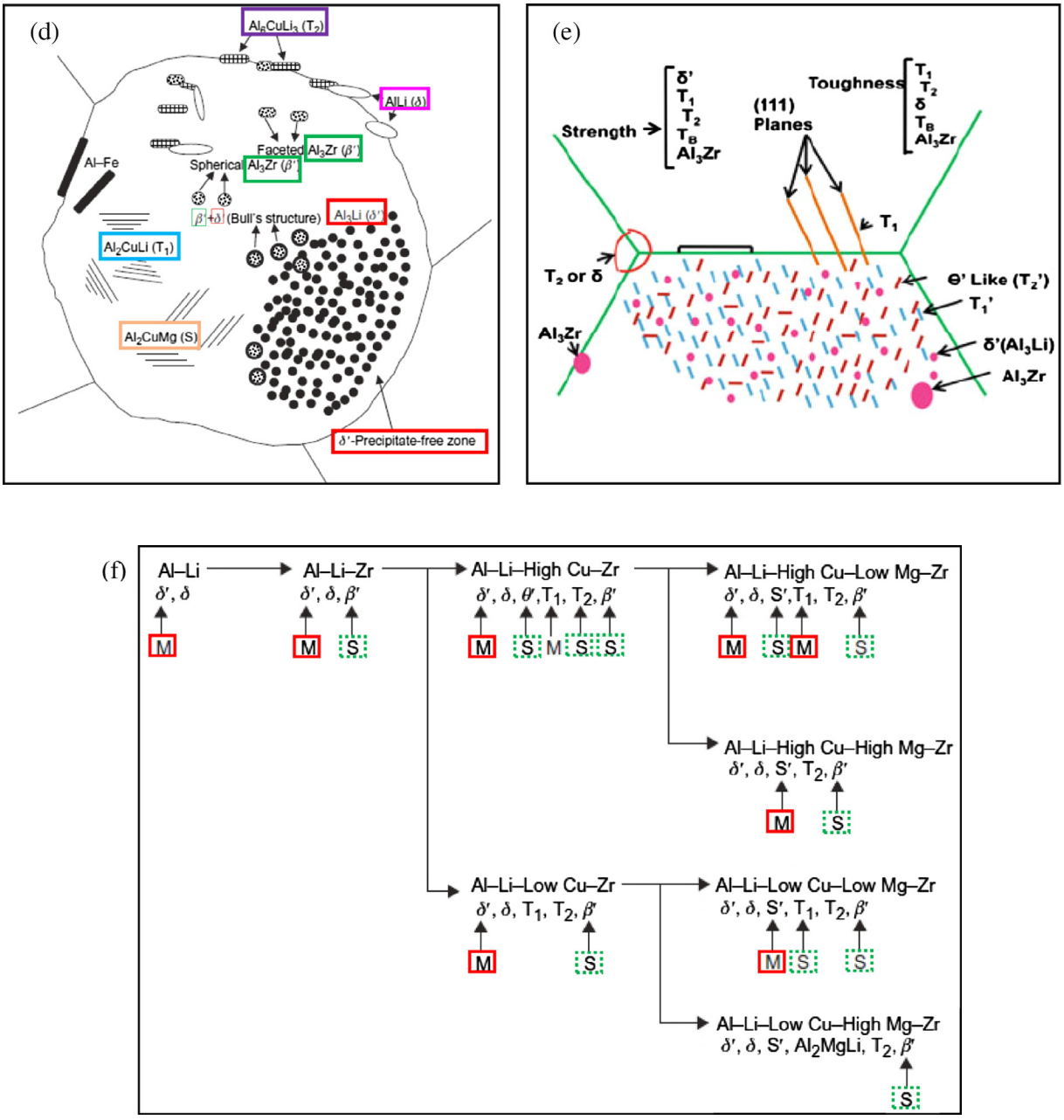

Fig. 5 (*continued*)

$$\tau_{CRSS} \propto (\gamma^{APB})^{\frac{3}{2}} \cdot ((\boldsymbol{r} - \boldsymbol{n_d} \cdot \boldsymbol{b_v}))^{1/2} \cdot \boldsymbol{f}^{\frac{1}{2}} \quad (2)$$

Therefore, minimizing τ_{CRSS} is crucial, in order to make further slip on that certain plane, so the slip is preferred to become planar, besides, the particular plane on which repeated slip takes place levelly becomes softened [66].

The degree of strengthening achieved from these mechanisms is varying with the chemical composition and the ageing condition of the alloy [3]. For example, in case of under-aged condition (the early stages of age hardening), the strengthening of Al-Li alloys is caused by synergy of modulus hardening, coherency strain hardening, and hardening from interfacial energy. However, for the peak-aged condition, the strengthening is created by modulus hardening and order hardening, besides, the dominant deformation behavior is planar slip deformation behavior [66–68]. In addition, the strengthening obtained from grain size and solid solution strengthening mechanisms at different ageing conditions was observed to be marginal as shown in Fig. 5a [68].

Although, Al_3Li has a great contribution on strengthening Al-Li alloys, it has been met with only limited success [69]. Therefore, other alloying elements such as Cu and Mg were added to Al-Li alloys to produce other strengthening phases, since the different amounts of these elements to Al-Li alloys has been displayed to be efficient in strengthening [3,8]. Cu and Mg contribute to improve the precipitation order either by forming Cu and Mg-based phases and co-precipitating with the Al_3Li or by altering the solubility of the principal alloying elements [68]. In addition, they can interact also with Li to precipitate as strengthening phases which occurred in quaternary (Al-Li-Cu-Mg) and the ternary (Al-Li-Cu) alloys. In Al-Li-Cu alloys, extra strengthening phases were obtained by co-precipitation of Cu-based phases individually of Al_3Li precipitation such as Al_2CuLi (T_1) and Al_6CuLi_3 (T_2) [3,68].

On the other hand, for Al-Li-Cu-Mg alloy the strengthening is caused by co-precipitating with Al_3Li and interacting with Li to produce more complex strengthening phases [66]. Adding Mg to Al-Li alloys creates Al_2CuMg (S') near grain boundaries (GBs) which leads to reduce/eliminate the precipitation –free zones (PFZs). Reducing PFZs is beneficial to avoid early failure and improve the strength of Al-Li alloys, since, the combinations of coarse grain boundary precipitates and PFZs allow the localized slip to create stress concentrations which nucleate voids at the grain boundary precipitates as shown in Fig. 5b [66–69]. In addition, the strengthening phases observed in Al-Li-Cu and Al-Li-Cu-Mg alloys are presented in Fig. 5c

Al_2Cu (θ') and Al_2CuLi phases were nucleated on the interface of Al_3Zr phase in Al-Li alloys, which have low amount of Zr. Although, the nucleation degree of Al_2CuLi is lower than Al_2Cu precipitates, the Al_2CuLi has a great impact on the elastic modulus of Al-Li alloys. The existence of Al_2CuLi precipitates is important for strengthening, since they act as un-shearable barrier that must be avoided by dislocations during deformation. It was reported that the strengthening phases, which precipitated from the solid solution are mainly based on the ratio of Cu and Li (Cu: Li). For example, if the Al-Li alloys contain high Li content (>2 wt%) and low Cu content (<2 wt%), the Al_2Cu strengthening precipitates will be suppressed and Al_2CuLi phase will occur. Further details for the effect of alloying elements on the Al-Li alloys are listed in Table 4, where, Li, Mg, Cu, Zr, Mn, and Ti have positive impacts on Al-Li alloys. However, Fe, Si, Na, and K have negative influence on Al-Li alloys [3,8]. The summary of different strengthening phases existed in several Al-Li alloys are graphically represented in Fig. 5d, e, and f. As shown in Figs., the Al–Li–Cu–Mg–Zr alloys showing complex strengthening phases, especially the Al–Li-low-Cu-high-Mg–Zr 3rd generation alloys, which are widely used in the commercial applications. Therefore, it is somehow difficult to optimise the microstructures using commercial processing technologies to obtain a good balance of engineering properties for these alloys.

Interaction modes between dislocations and Al_3Li

The possible interaction modes between dislocations and Al_3Li are depicted in Fig. 6 [70]. The shape of the dislocations mainly relies upon the size and volume fraction of Al_3Li. For the Al-Li alloys under aged or peak-aged conditions, the dislocations move in pairs because of fine precipitates (particles) of Al_3Li occur [66,70]. The first dislocation demolishes the forms and order of APB in the Al_3Li precipitates. However, the second dislocation may remove the disorder caused by the first dislocation [71]. It is almost a straight when only very fine precipitates of Al_3Li form as depicted in Fig. 6a. On the other hand, as shown in Fig. 6b, the dislocations are progressively bowing out between Al_3Li precipitates with the growth of precipitates [70,71]. As shown in Fig. 6c and d, with more growth of precipitates, the dislocation becomes wavy, in which, the length of wave, the separation of dislocations in pairs, and the curvature of the bowed out dislocations are obviously relied on the distribution of Al_3Li [70]. It is worth mentioning that for Al-Li alloys under peak-aged condition, the dislocations exist in the matrix keeping out of Al_3Li [71]. As presented in Fig. 6c, the separation distances of the dislocations in pairs are approximately two times higher than the precipitates size [70]. As shown in Fig. 6d, when the precipitates grow more, the dislocation bypass the precipitates and leave dislocation loops around particles, which decreases the strength of the alloys [70]. The relationship between strength and the size of the second phase particles is depicted in Fig. 6e, in which, the precipitates which possess a radius less than a critical size (critical radius) might be sheared by the dislocation pairs. However, with the growth of precipitates (radius of precipitates more than critical radius), bowing or bypassing may occur [70,71].

Table 4
The impacts of alloying elements on Al-Li alloys [3,66].

Alloying elements	Effect
Li and Mg	• Solid-solution strengthening • Precipitation strengthening • Decrease density
Cu and Ag	• Solid-solution strengthening • Precipitation strengthening
Zn	• Solid-solution strengthening • Improve corrosion properties
Zr and Mn	• Texture control • Govern of recrystallization
Ti	• Considered as grain refiner during ingots solidifications
Fe and Si	• Considered as impurities affecting fatigue, corrosion properties and fracture toughness
Na and K	• Considered as impurities affecting fracture toughness.

Deformation behavior of Al-Li alloys

The factors that cause a negative effect on the tensile deformation and formability in Al-Li alloys have the same effect on the fracture resistance and toughness of these alloys. These factors are introduced as follows:

(1) Planar deformation and strain localization because of the Al_3Li phases shearing, causing premature fracture near the grain boundaries [58,70–74]
(2) Slip localization on the Al_3Li precipitate-free zones (PFZ) created during artificial ageing [75]
(3) Coarse equilibrium phases, such as AlLi, Al_2CuLi, and Al_6CuLi_3, and the coarse Fe-rich and Si-rich intermetallic phases adjacent to the grain boundaries [76,77]
(4) Separation of potassium (K) and sodium (Na) in the grain boundaries and the creation of fine-film eutectic phases adjacent to the grain boundaries [78,79]
(5) Grain boundary embrittlement, which is attributed to a high hydrogen content [80]
(6) Crack propagation on the sub-grain and grain boundaries, especially in un-recrystallized alloys [81].

In this review, we will focus only on factors (1) and (2), since, the dominant deformation behavior of Al-Li alloys (notably aged Al-Li alloys) is planar slip deformation behavior [66–68].

Planar slip deformation characterization

Shearing of the strengthening phases causes the accumulation of dislocations on the grain boundaries and adjacent to the grain boundary triple junctions, which increases the number of precipitates or the grain size. The number of dislocations that accumulate across the grain boundaries increases as the number of strengthening precipitates that can easily shear increases. This increase creates significant slip lengths and higher "local" stress concentrations on both the grain boundaries and the grain boundary triple junctions, as schematically depicted in Fig. 7a.

The micro-void and micro-crack nucleation should occur along the intersections of the slip bands and grain boundaries, and the consolidation of these nucleation locations can cause intergranular

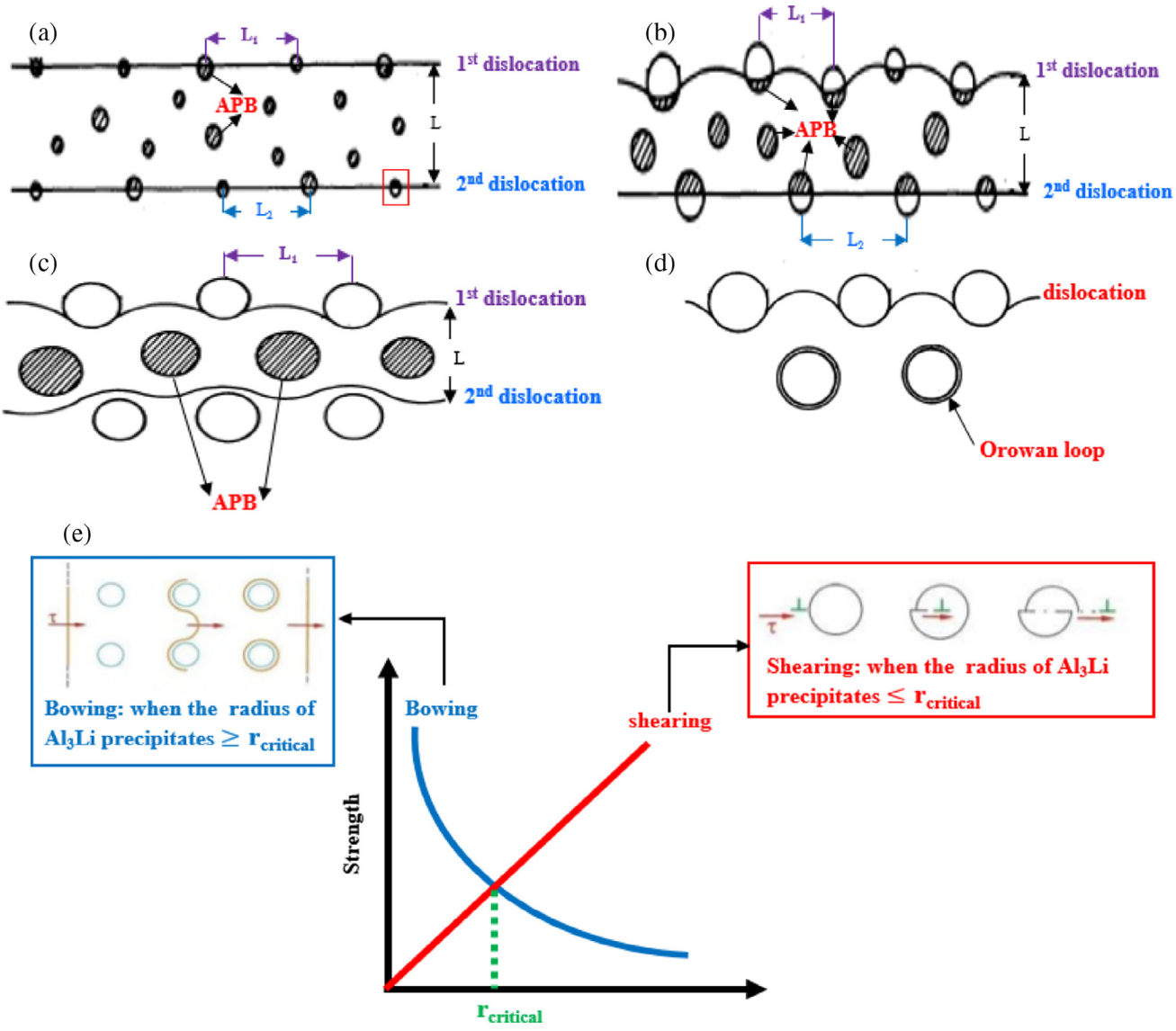

Fig. 6. Schematic representation of the interaction modes between ordered precipitates of Al_3Li and dislocations, in which the textured areas describe APB. (a) As-quenched condition [70]; (b) Under-aged condition [70]; (c) peak-aged condition [70]; (d) over-aged condition [70]; (e) The comparison between bowing and shearing mechanisms as a function of precipitates size (critical radius). L is the separation distance between the 1st and 2nd dislocation, besides, L_1 and L_2 are the particle spacing for the 1st and 2nd dislocation.

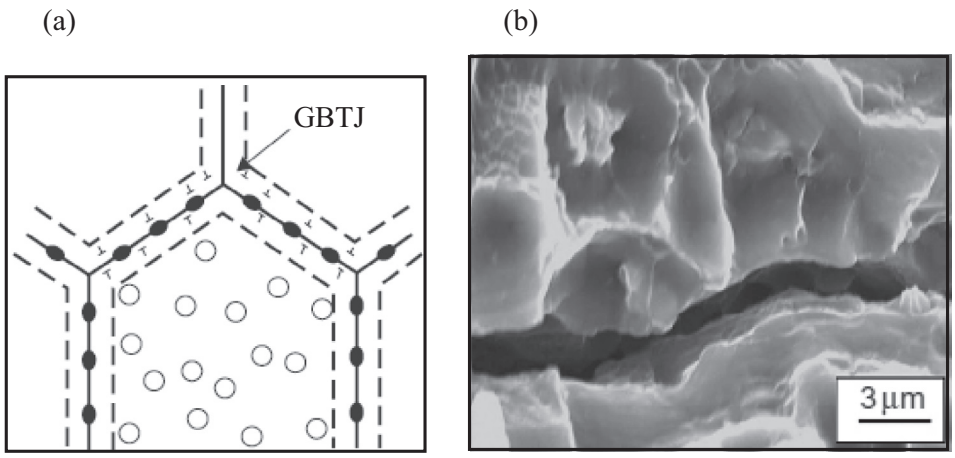

Fig. 7. (a) Schematic depicting precipitate-free zones (PFZ) at grain boundary and accumulation of a stress concentration on Grain boundary triple junction (GBTJ) [66]; (b) SEM depicting intergranular fracture and a population of micro-voids along to the grain boundary crack for AA 8090 Al-Li alloy [66].

fracture, as shown in Fig. 7b [66,75,82]. Similar planar slip deformations have been observed in other precipitation-hardened Al alloys, but the influence is exceptionally serious in Al-Li alloys due to the improvement in the strain localization on both the grain boundaries and grain boundary triple junctions caused by the Al_3Li PFZs. The improved strain localization promotes a generous "localized" deformation that occurs before the macroscopic deformation [82–84]. When the localized deformation is linked to the "local" stress concentrations and the associated micro-void or micro-crack nucleation in the intermediate and coarse grain intermetallic phases, the result is poor ductility and fracture toughness [84,85].

Planar slip and strain localization solutions

Adjusting the deformation mode from dislocation shearing of the strengthening phases to bypass the strengthening phases can reduce the strain localization in the alloy matrix. However, the strain localization is complex in Al-Li alloys due to the small strains associated with the Al_3Li strengthening phases, and the size of the precipitates increases before becoming non-coherent. This leads to a notable growth in the PFZs and decreases in the tensile ductility and fracture toughness. Therefore, over ageing is not readily useable to promote and/or induce slip homogenization. Three other methods to accomplish this include:

(a) reducing the grain size [83];
(b) controlling the recrystallization degree [83,84]; and
(c) adding alloying elements, such as Mg and Cu, to create non-shearable strengthening phases [85].

Methods (a) and (b) depend on reducing the slip length so the local stress concentrations are caused by the dislocation accumulations. Methods (a) and (b) take advantage of adding grain-refining components, which result in reduced grain growth, a small grain size, a decrease in the recrystallization degree and an influence on the slip dispersal. Using methods (a) and (b), notable increases in the tensile properties, formability, and fracture toughness can be obtained due to the change in the fracture mode from intergranular to trans-granular shear fracture, but the anisotropy in the tensile properties is the main shortcoming of these methods due to the un-recrystallized microstructure being retained, particularly in sheet products [86]. Therefore, method (c) is recommended to overcome the disadvantage of anisotropy in the tensile properties [72,86].

The addition of alloying components, such as Mn and Zn, creates non-sharable strengthening particles that caused the cross-slip. An insignificant increase in the tensile properties was observed, and the strength was significantly reduced. A reduction in the volume fraction of the Al_3Li strengthening phases is the main reason for the undesirable behavior [72].

The best solution for a planar slip in Al-Li alloys has been reported to be the addition of Mg and Cu alloying elements, which create non-shearable Al_2CuMg strengthening precipitates [72]. As mentioned in this review, the alloy matrix slip planes are not parallel to the slip planes in the Al_2CuMg strengthening precipitates; therefore, the dislocation shearing paths of the Al_2CuMg strengthening precipitates through the alloy matrix are obstructed. The reduction in the slip localization and improvement in the local work hardening are attributed to the bowing dislocations near the Al_2CuMg strengthening precipitates. However, a uniform and dense dispersion of Al_2CuMg strengthening precipitates is necessary to efficiently create and/or cause slip homogenization at the fine microscopic level [72,86–89]. This method can create isotropic properties in highly textured Al-Li alloys [89]. Fig. 8a and b depict the positive influences of the Al_2CuMg strengthening precipitate distribution on the ratio of the tensile to yield strength and elongation, respectively.

Anisotropic behavior of the Al-Li alloys

The properties of the former Al-Li (1st and 2nd generations) alloys do not satisfy most of the design and manufacturing requirements because of their vital shortcomings, such as their anisotropic tensile properties, poor formability and fracture toughness, low corrosion resistance, formation of micro-voids and micro-cracks during processing, and crack deviation [1,3]. Therefore, the 3rd generation of Al-Li alloys was created to overcome the disadvantages of the former generations and to meet the requirements of manufacturers and designers [3]. Anisotropic behavior is the most critical shortcoming in the Al-Li alloys (especially those predominantly containing un-recrystallized grains) because it has a critical negative effect on the final product quality and cause various problems, such as earing as shown in Fig. 9a and b [90]. Therefore, comprehensive efforts have been devoted to developing practical methods

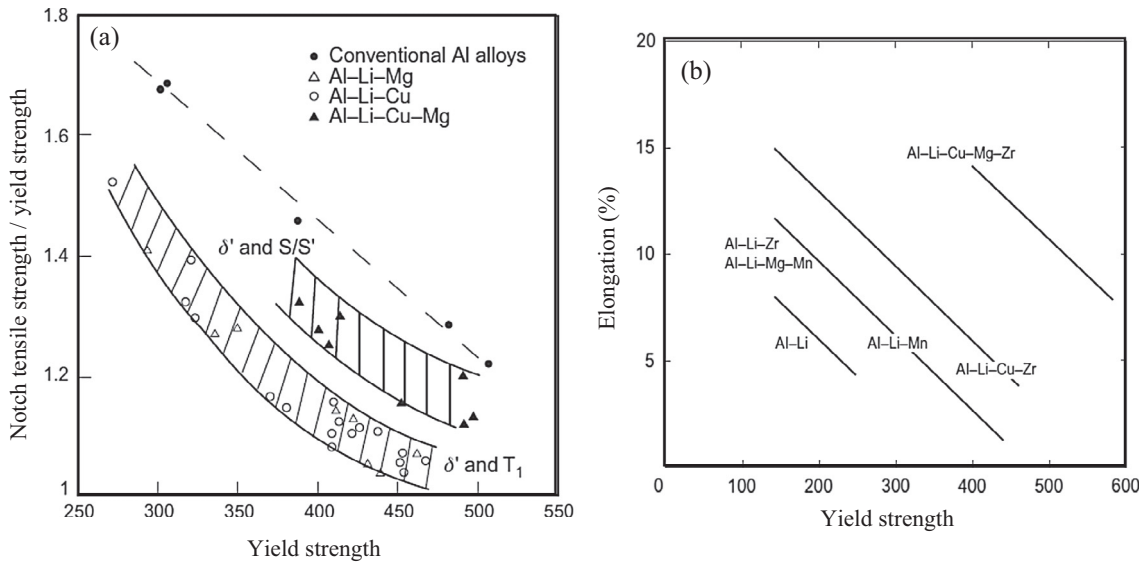

Fig. 8. The effect of Al_2CuMg precipitates on (a) both of tensile and yield strengths for Al-Li alloys [66]. And (b) on elongation and yield strength [5].

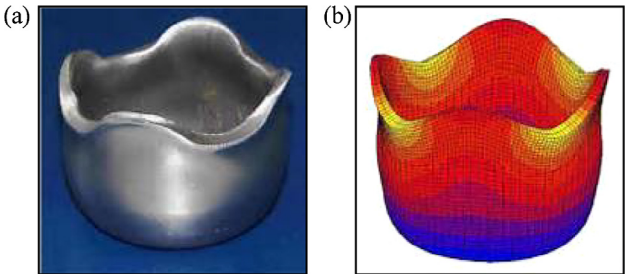

Fig. 9. (a) Experimental and (b) Finite Element simulation of deep drawn cup showing earing defect due to anisotropic mechanical properties [90].

to decrease the texture and anisotropy in Al-Li alloys to increase the ease of design and forming [2,3,5].

The main reasons for the anisotropic tensile properties are the following [91–94]:

(a) The crystallographic texture, which is defined as the alignment degree of each grain in a polycrystalline metal
(b) The characteristics of the main strengthening phases
(c) The fibre orientation, which includes the grain shapes (widths and aspect ratios); fine grain banding; equilibrium phases; other precipitates in the microstructure; and the alignment of intermediate and coarse intermetallic phases

The effects of the crystallographic texture on Al alloys, especially those that contain an isotropic face-centred cubic (FCC) structure, are not strong. However, Al-Li alloys, notably 2nd generation alloys such as AA 8090, AA 2090 and AA 2091, frequently show strong anisotropic tensile properties (through the thickness and in-plane anisotropy). It was reported that, S, copper, and brass texture components were observed during the thermomechanical processing of Al and Al-Li to produce sheets, plates and extruded products [94]. However, the brass texture component in Al-Li alloys is higher than the brass component in Al alloy. This means that degree of anisotropic behavior of Al-Li alloys is higher than the anisotropic behavior in Al alloys since the existence of brass texture component is the main reason for anisotropic behavior in these alloys [5,66,94]. Usually, Al and Al-Li alloys display a string of texture orientations from brass $\{110\}\langle 112\rangle$ component, through the S $\{123\}\langle 634\rangle$ component to the copper $\{112\}\langle 111\rangle$ component [94].

Recently, some studies reported that pre-stretching prior to artificial ageing, developing the recrystallization degree, and ageing over the max strength can be used to reduce the anisotropic tensile properties of former Al-Li alloys [3,4,94,95]. The anisotropic tensile properties are minimized by the previous approaches, but these approaches also affect other properties and cause various difficulties during manufacturing. These difficulties decreased the competitiveness of former Al-Li alloys as substitutes for traditional Al alloys. The anisotropic tensile properties that hindered the 2nd generation alloys were widely investigated during the development of the 3rd generation alloys. The development of the 3rd generation Al-Li alloys was based on reducing the Li content ($Li < 2$ wt%) and using new approaches, such as controlling the recrystallization degree and deformation texture by adding alloying elements (Mn, Zr) and using novel thermomechanical processing (TMP). These approaches or methods significantly influence the anisotropic tensile properties [5,66]. The key points controlling the tensile properties and anisotropy of selected Al-Li alloys will be discussed in the next section.

The anisotropy in sheet metal is typified by the r-value (Lankford parameter). Hill (1950) reported that the r-value can be characterized using equations (3–6). For the quasi-static uniaxial tensile test, two independent extensometers are placed on the samples to simultaneously determine the longitudinal (ε_l) and transverse (ε_w) strains. However, for the high strain rate (dynamic) tensile test, the r-value are calculated using the method introduced by [1,96]. The plastic longitudinal and width strains can be obtained from grids printed on the surface of the sample. During the dynamic test, the shapes of the rectangular grids continuously change due to deformation, as shown in Fig. 10. The grid pattern is parallel to the direction of the uniaxial tension. A high-speed camera can be used to measure and detect gauge length deformations in the grid, and the plastic longitudinal, width and thickness strains can be calculated using the tested samples.

$$r = \frac{\varepsilon_w}{\varepsilon_t} \tag{3}$$

$$\varepsilon_t = -(\varepsilon_l + \varepsilon_w) \tag{4}$$

$$r = -\frac{\varepsilon_w}{(\varepsilon_l + \varepsilon_w)} \tag{5}$$

$$r = \frac{\ln\left(\frac{y_2}{y_1}\right)}{\ln\left(\frac{x_1 y_1}{x_2 y_2}\right)} \tag{6}$$

where $\boldsymbol{r}$ is the anisotropic parameter (Lankford parameter), $\boldsymbol{\varepsilon_l, \varepsilon_w, \varepsilon_t}$, are thickness, longitudinal, and width strains respectively and $\boldsymbol{x_1, y_1, x_2, y_2}$ are length of the rectangle grid on x and y-directions before and after tensile test respectively.

Tensile properties of AA1420: A 1st generation Al-Li alloy

As previously mentioned, in the early 1960s, various studies were performed by researchers in the former Soviet Union to develop new alloys without the disadvantages of AA2020 and with new advantages to fulfil the requirements of designers and manufacturers. One of these developed alloys, AA1420, has one of the lowest densities available in commercial alloys [57,59]. Although AA1420 alloy offers superior properties, such as a low density and good weldability and stiffness, its yield, tensile strength and fracture toughness are not sufficient to fulfil the requirements of modern space applications. In addition, AA1420 suffers from anisotropic tensile properties, which lead to serious problems in product manufacturing and quality. Al_3Li shearing, which causes planar slip, is the main strengthening phase in Al-Li alloys and is the main

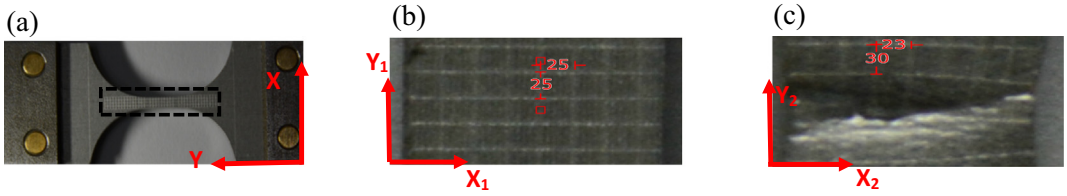

Fig. 10. (a) sample with rectangle grids market on its surface before test; (b) grids before, (c) grids after dynamic test.

reason for the poor formability and fracture toughness. Furthermore, the recrystallization degree and deformation texture are the principal reasons for the anisotropic tensile properties. Therefore, further investigations examined the alloy composition to obtain additional non-shearable phases and to control the recrystallization degree and deformation texture that decrease the planar slip tendency and reduce the anisotropy in the tensile properties [54–57].

The stress-strain curves of AA1420 at room temperature with different loading conditions (i.e., 0°, 45°, and 90°) and strain rates (0.001 s^{-1} and 0.01 s^{-1}) are depicted in Fig. 11a and b. In order to determine the tensile properties, such as the strain hardening exponent (n), flow stress (FS), ultimate tensile stress (UTS), and elongation to fracture (El.%), Swift equation (Eq. (7)) was fitted to the stress-strain data for each tested specimen, where, each test condition was examined with at least three specimens.

$$\boldsymbol{\sigma_y} = \boldsymbol{K}(\boldsymbol{\varepsilon_0} + \boldsymbol{\varepsilon_p})^{\boldsymbol{n}} \quad (7)$$

where $\boldsymbol{\sigma_y}$, $\boldsymbol{K}$ and $\boldsymbol{n}$ are yield stress, strength coefficient and strain hardening index respectively, as well as, $\boldsymbol{\varepsilon_0}$ and $\boldsymbol{\varepsilon_p}$ are strain offset constant and plastic strain respectively.

As depicted in Fig. 11c, and d, the FS and UTS values for RD are higher than those for the 45° and 90° directions. As well, the El.% for TD was higher than that for the RD and 45° directions, as shown in Fig. 11e. These results show that the AA1420 tensile properties vary in relation to the direction from the RD, which signify that AA1420 exhibits anisotropic behavior and suffers from anisotropy in its tensile properties. Moreover, we have investigated the effect of strain rate on tensile properties and anisotropic behavior of AA1420, since strain rate has a significant effect on the tensile properties of the metal sheets. We will discuss the impacts of strain on tensile properties of AA1420, AA8090 and AA2060 in the subsequent section.

Tensile properties of AA8090: A 2nd generation Al-Li alloy

The stress-strain curves of AA8090 at room temperature with different orientations and strain rates (0.001 s^{-1} and 0.01 s^{-1}) are depicted in Fig. 11a and b, respectively. We have noticed that the tensile properties of AA8090 were dependent on the loading directions, where, the FS and UTS values for RD are higher than those for the 90° and 45° directions (Fig. 11c, and d). Besides, the El.% for TD was higher than that for the 45° and RD and directions, as depicted in Fig. 11e. This means that AA8090 displayed anisotropy in its tensile properties. Moreover, the degree of anisotropy in the tensile properties of AA8090 was higher than that in AA1420, the finding which is in line with those reported in previous investigations [97–99]. Anisotropic tensile properties (through-thickness anisotropy and in-plane anisotropy) are a pivotal issue that has received much attention in 2nd generation Al-Li alloys, particularly anisotropy in the ductility, yield, ultimate strength and fracture toughness as depicted in previous figures. Most of the 2nd generation Al-Li alloy plates have lower yield stresses on the surface of the plates than in the midsection [3,6,100,101].

Indeed, the anisotropic tensile properties of former Al-Li alloys (1st and 2nd generation) are very complex because the alloys are affected by the crystallographic texture and other factors such as the sizes, shapes and orientations of the grains and sub-grains, the grain size gradients, the shape and orientation of the strengthening phases, and the dislocation structure. Thus, the anisotropic tensile properties are related to the crystallographic texture and the texture or anisotropy due to precipitate dislocation interactions. Therefore, various investigations have attempted to model the yield stress anisotropy from a purely crystallographic perspective. For instance, relaxed-constraint models have been developed to determine the grain morphology, but the agreement between the predictions and observations was not good [102]. The viscoplastic self-consistent model (VPSC) was used in this study to model the anisotropy in the yield stress of the AA2090 alloy (heat-treated solution conditions) to overcome the effects of strengthening precipitation [103]. The results predicted by the VPSC model were better than the results obtained by the Taylor model, but the modelling should be improved by adding microstructural parameters. Accordingly, investigations have been performed to determine the relation between the crystallographic texture and the anisotropy in the tensile properties and to explain the influence of the strengthening phases and slip nature on the rolling texture evolution of Al-Li alloys [104–108]. For instance, the yield function suggested by Bron and Besson was developed to model the anisotropy observed in the yield and to explain the difference in the Lankford coefficient (r-value). The simulation results from this investigation well agreed with the experimentation results [109,110].

The influence of the strengthening phases on the tensile properties is attributed to the formation of special crystallographic planes and their subsequent interactions with dislocations. Thus, the relations of the orientation, shape, size and distribution of the strengthening phases within the alloy matrix are vitally important. The main characteristics that affect the mechanical properties of previous generation Al-Li alloys and lead to anisotropy in the tensile properties are summarized in Table 5 [109–119].

Tensile properties of AA2060: A 3rd generation Al-Li alloy

AA2060 is a 3rd generation Al-Li alloy that was created by Alcan Inc. in 2011 to manufacture fuselage/pressure cabins, lower wings, and wing/fuselage forgings instead of a traditional Al alloy, as depicted in Fig. 4 and Table 3. The nominal composition and density of AA2060 are listed in Table 1. The stress-strain curves of AA2060-T8 are depicted in Fig. 11a and b at room temperature with different orientations and strain rates (0.001 and 0.01 s^{-1}). The effect of loading direction on FS, UTS, and El.% of AA2060 is depicted in Fig. 11c, d, and e. We have noticed that the FS and UTS in RD and 90° are higher than in 30°, 45°, and 60°. Besides, El.% in 45° and 60° are higher than RD and 90°. This indicates that AA2060 still suffering from anisotropy in their tensile properties. However, the degree of anisotropy in the tensile properties of AA2060 was low compared with that of AA1420 and AA8090. The reasons for the anisotropic tensile properties and the factors affecting and controlling the mechanical behavior and formability of AA2060 have seldom been investigated. Additionally, the dominant deformation mechanisms and fracture behavior of this alloy under wide range of temperature and strain rate have not been explored. Therefore, the authors recently began studies to explore and address the abovementioned issues and challenges.

Influence of strain rate on tensile properties and anisotropic behavior of AA1420, AA8090, and AA2060 at rolling direction (RD)

Understanding the effect of strain rate on the tensile properties (i.e. FS, UTS, n, and El.%) is crucial to control the forming process as well as govern the properties of the final product. As shown in Fig. 12a (for AA1420 and AA8090), while strain rate increases, the FS and UTS are slightly decreased till strain rate of 0.1 s^{-1}, increased gradually up to strain rate of 100 s^{-1}, and finally drop at strain rate beyond 100 s^{-1} to 2000 s^{-1}. For AA2060 alloy, increasing the strain rate resulted in slightly decreases of FS and UTS until strain rate reaches to 0.1 s^{-1} and gradually increases up to strain rate of 10 s^{-1} and declines at strain rate after 10 s^{-1} to 2000 s^{-1}. As depicted in Fig. 12b, we observed that both n and El.% were increased up to strain rate of 0.1 s^{-1} and decreases gradually till strain rate reaches

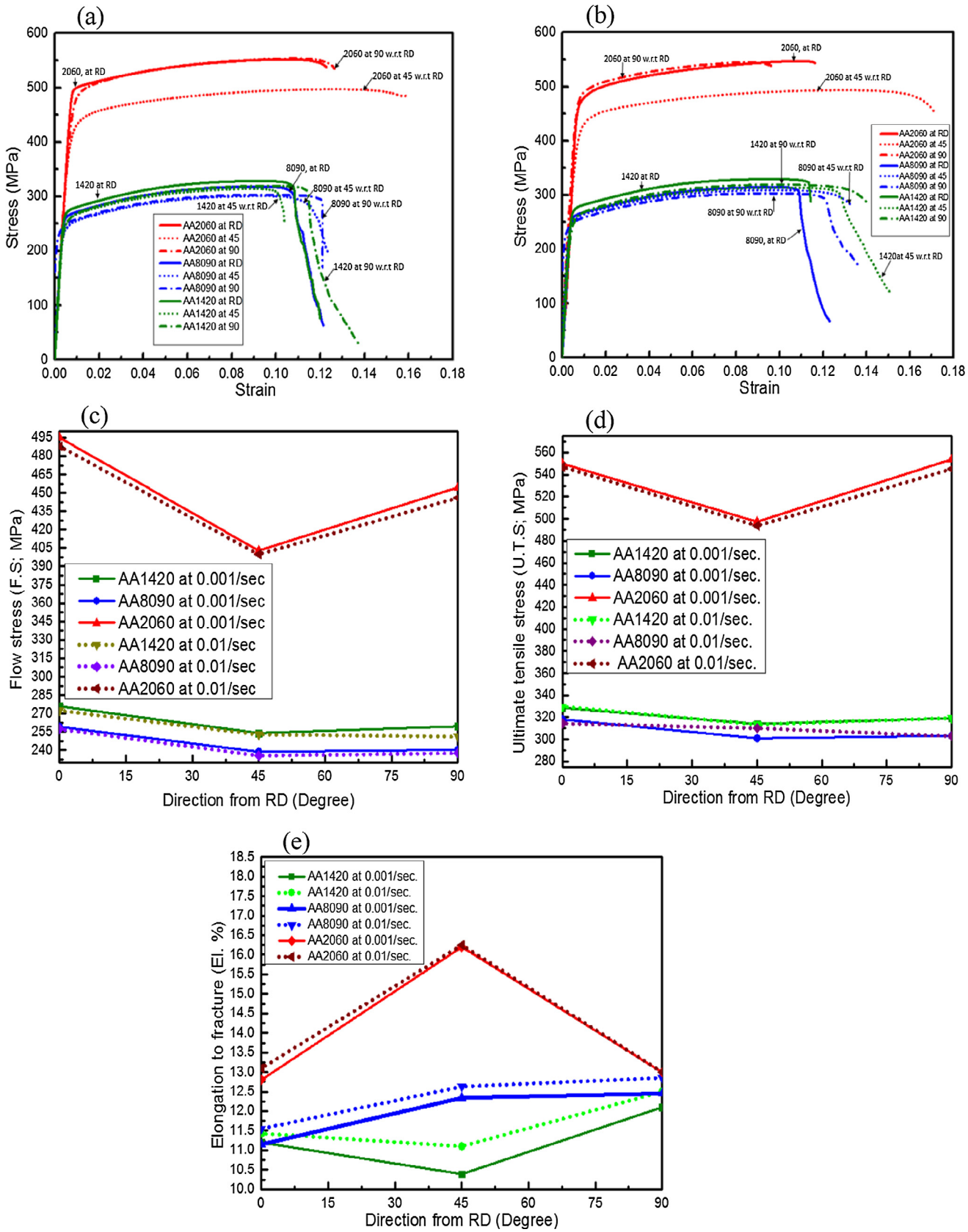

Fig. 11. Stress-strain curves of AA1420, AA8090 and AA2060 sheet at (a) $\varepsilon = 0.001\ s^{-1}$ and (b) $\varepsilon = 0.01\ s^{-1}$ and different loading directions; variation in (c) flow stress, (d) ultimate tensile stress; and (e) Elongation to fracture% in relation of loading direction (0°, 30°, 45°, 60°, and 90° w.r.t. RD) for AA1420, AA8090 and AA2060 at $\varepsilon = 0.001$ & 0.01/s.

Table 5
The main factors causing anisotropy in ductility, yield strength and ultimate tensile strength of Al-Li alloys [109–119].

Tensile property	Reasons for anisotropy
Ductility [109–113]	• Shearing of the Al_3li phases and the resultant flow localization orientation w.r.t the current stress states • Distribution and density of the intermediate and coarse grain size of intermetallic phases • Type, distribution and morphology of the main strengthening phases, which are governing by alloy alloying addition and TMP • Recrystallization degree, type and history of deformation process before artificial ageing • Fracture modes • Strength of grain boundaries • The width of PFZs • Equilibrium phases densities along the grain boundaries
Yield Strength [112–117]	• Crystallographic texture • Final heat-treatment condition • The degree of recrystallization • Solution heat treatment caused a higher degree anisotropy in yield strength correlated to the artificial ageing condition • Nature and Distribution of strengthening phases
Ultimate tensile strength (the degree of anisotropy in ultimate tensile strength is lower than the anisotropy in yield strength) [114–119]	• The degree of recrystallization • Nature and Distribution of strengthening phases • Resultant microscopic deformation behavior

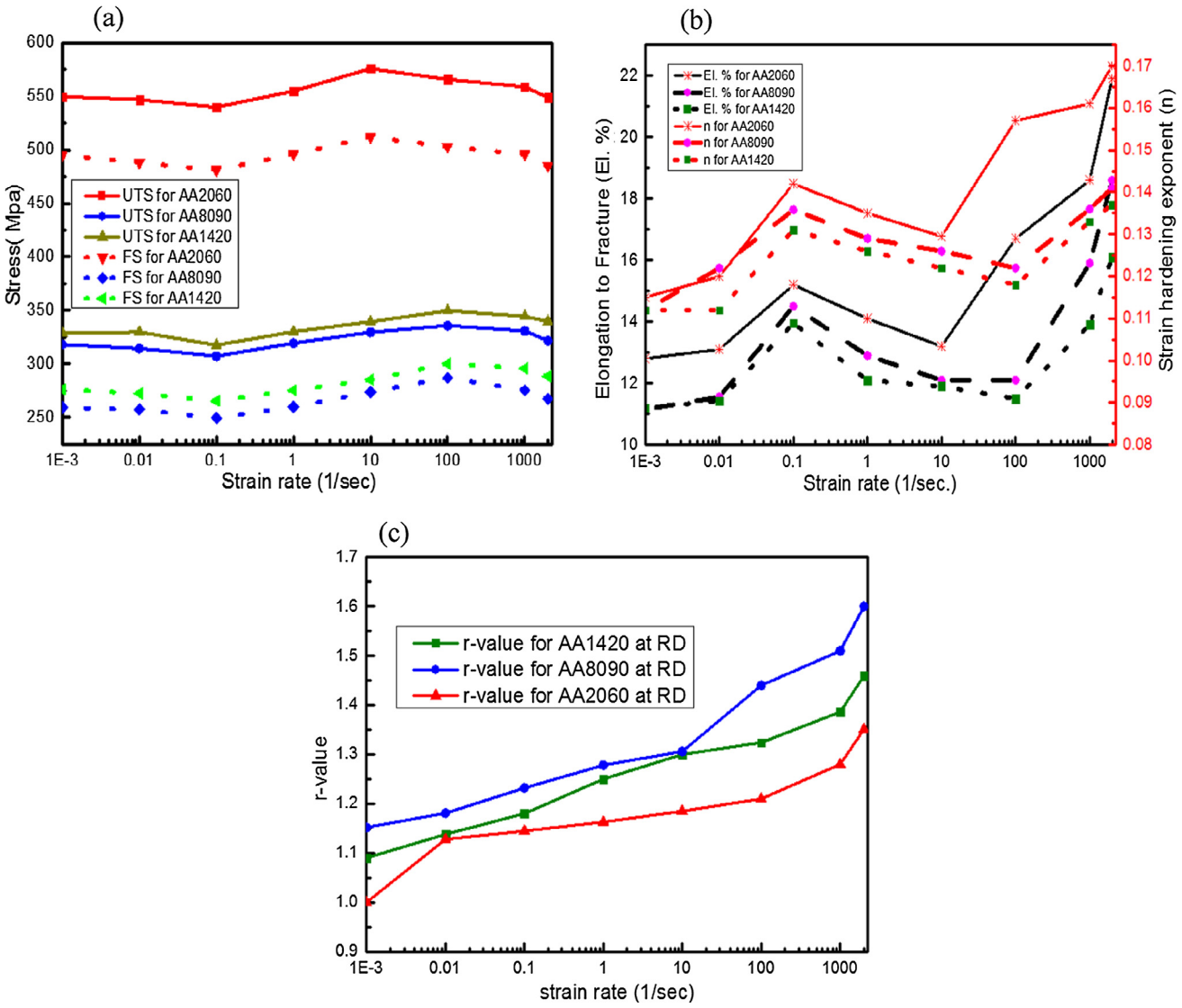

Fig. 12. Variation in (a) flow and ultimate tensile stresses; (b) elongation to fracture% and strain hardening exponent; and (c) r-values of AA1420, AA8090 and AA2060 in relation of strain rates (0.001–2000/s).

Table 6
The practical approaches and their effects on crystallographic texture and anisotropy of Al-Li alloys.

Practical method	Effect
Reduce the amount of Zr by adding another alloying element for grain refining instead of it [120]	• Reducing the influences of Al3Zr phase (which offered a strong rolling texture) in avoiding and pining recrystallization and grain boundaries respectively • Decreasing or replacing the amount of Zr with Cr and Mn will form (Cr + Mn) - phase that offers an apparently weak texture
Over-ageing before Material processing step [72]	• Material processing such as hot, warm or cold forming process causing homogeneous slipping all along processing. This lead to reduce the amount of brass texture and consecutively decrease the degree of anisotropy in Al-Li alloy sheets • Although Over-ageing can reduce anisotropy in tensile properties successfully for Al-Li alloy, it has a negative effect on fracture toughness (reduce fracture toughness), therefore this approach cannot be used to reduce anisotropy in tensile properties for the products required high toughness
Solution treatment subsequent with Stretching in direction orientation w.r.t rolling direction [120]	• This will lead to align the strengthening phases not only on rolling direction but also in other directions w.r.t rolling direction
The amount of deformation process [101,120,121]	• Decreasing the amount of deformation during hot forming lead to prevent the texture sharpness
Recrystallization in-between processing steps[101]	• Reducing the comprehensive texture intensity

100 s^{-1}, and sharply increased at strain rate range of 100 s^{-1} to 2000 s^{-1} for AA1420 and AA8090. At the same time, for AA2060, n and El.% were increase till strain rate of 0.1 s^{-1} and decreases constantly till strain rate reaches 10 s^{-1} and clearly increased at strain rate beyond 10 s^{-1} to 2000 s^{-1}. These results imply that the formability of AA1420, AA8090, and AA2060 can be increased and improved by increasing strain rate. As shown in Fig. 12b, El.% for AA1420 and AA8090 at a strain rate of 1000 s^{-1} and above is much higher than the El.% at a strain rate before 1000/s. In addition, the El.% for AA2060 at a strain rate of 100 s^{-1} and beyond was much higher than El.% at a strain rate before 1000 s^{-1}. In reference to the relation between formability and El.%, the formability for AA1420, AA8090, and AA2060 may be increased remarkably at a high rate of deformation due to an improvement of El.%, in particularly, AA2060 which displays good El.% at high strain rates compared with that of AA1420 and AA8090.

The variations of anisotropy (r-value) for AA1420, AA8090, and AA2060 are shown in Fig. 12c in respect to strain rate at RD. It is noted that the r-values of AA8090 are slightly higher than those of AA1420 and AA2060 till strain rate of 100 s^{-1} and then sharply increased up to strain rate 2000 s^{-1}. Hence, AA8090 expose a high anisotropy than AA1420 and AA2060 based on the anisotropic parameter. Even though, the anisotropy parameter (r-value) may be used to assess the formability in sheet metals, it is somehow difficult to investigate the effect of strain rate on the formability of sheet, in particularly at a high rate of deformation. The results obtained by quasi-static and dynamic tensile tests signify tensile properties do not display the constant trend as well as the formability cannot be ascertained. By comparing the tensile properties of these alloys, we observed that AA2060 alloy have superior tensile properties particularly in RD and TD.

Generally, the factors governing the anisotropic behavior and affecting the plastic response, deformation mechanisms and formability of Al-Li alloys notably at room temperature and under high strain rates conditions are rarely examined. Thus, it's vital to understand the micro/macroscopic response and deformation behavior of Al-Li alloys at wide range of temperature and strain rates in order to govern the forming processes and control the properties of the final components. Accordingly, the authors are trying to establish multi-scale models that capture the anisotropic response of Al-Li alloys at different forming conditions and link the microstructural state of Al-Li alloys with the mechanical performance. This leads to predict the mechanical behavior of Al-Li alloys and provide the macroscopic response with reference to microstructure parameters (grain size, shape and order distribution).

Practical methods for controlling the crystallographic texture of Al-Li alloys

Five methods have been identified to address anisotropy in the tensile properties of Al-Li alloys, and these methods and their influences on the anisotropic tensile properties are listed in Table 6. These methods successfully decrease the texture and reduce the anisotropy in lab-scale ingots and on an industrial level. For instance, recrystallization in-between processing steps (method 5) was successfully used to reduce the anisotropy in the tensile properties of lab-scale Al-Li ingots [120,62]. Afterwards, the lab-scale trials were scaled up to industry levels [3,5]. The fabrication chart proposed by Alcoa/AFRL to decrease the texture of thick Al-Li plates is depicted in Fig. 13a, and the general process flow chart proposed to produce un-crystallized Al-Li alloys sheets and plates with a low degree of brass texture is shown in Fig. 13b.

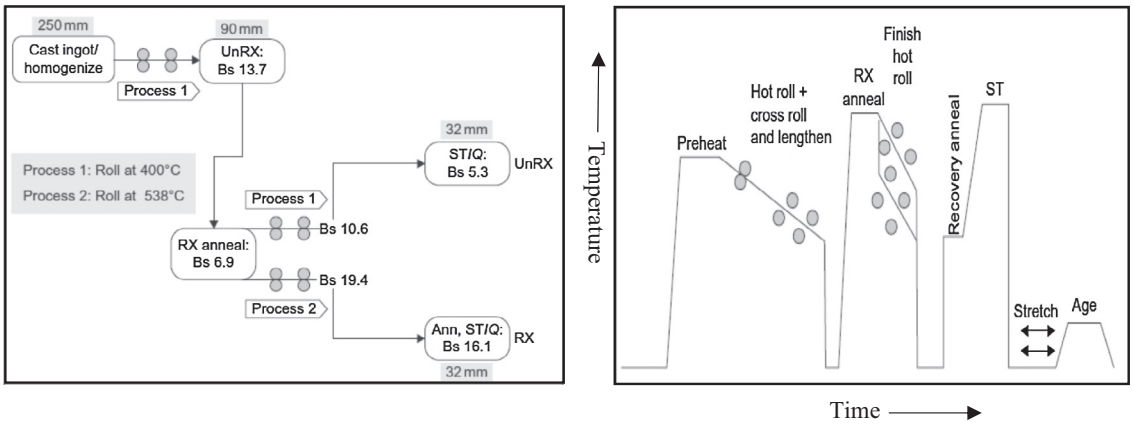

Fig. 13. (a) Fabrication chart proposed by Alcoa/AFRL to reduce the texture of Al-Li thick plates [62]; (b) general process flow chart for Al-Li alloy sheets and plates [3].

Conclusions

This review summarized studies that have been performed by researchers over the last few years on Al-Li alloys, notably, the strengthening mechanisms, anisotropic response and deformation behavior aspects. The main conclusions acquired from this review are summarized as follows:

- Al-Li alloys have attracted attention for use in weight and stiffness-critical structures for aerospace, and military applications because they exhibit superior properties compared with those of conventional Al alloys. Based on their production date, Al-Li alloys are classified into three generations, i.e., 1st, 2nd, and 3rd generation Al-Li alloys.
- Although the previous Al-Li alloys (1st and 2nd generations) exhibit exceptional properties, they do not meet most of the manufacturing requirements because of critical shortcomings such as poor formability and anisotropic tensile properties which is the main issue of former Al-Li alloys. Thus, the 3rd generation Al-Li alloys were developed to address the anisotropic behavior and other issues by optimizing the alloy composition and TMP.
- The main reasons for anisotropic tensile properties are: (1) crystallographic texture; (2) shearing of the Al_3Li phases and the resultant flow localization orientation relative to the current stress states; (3) type, distribution and morphology of the main strengthening phases, which are governed by alloying additions and TMP; and (4) recrystallization degree and type and history of the deformation process before artificial ageing.
- Although the 3rd generation Al-Li alloys offers superior properties compared with those of the previous Al-Li alloys, they still suffering from anisotropic tensile properties (the degree of anisotropy in these alloys is less than that in the former Al-Li alloys). Therefore, additional investigations are required to further improve and enhance the crystallographic texture, microstructure and damage tolerance and to reduce the anisotropic behavior.
- The main strengthening in Al-Li alloys is generally achieved from the existence of a huge volume fraction of the Al_3Li phase, which creates several mechanisms such as coherency and surface hardening, modulus hardening and order hardening. The degree of strengthening achieved from these mechanisms is varying with the chemical composition and the ageing condition of the alloy. Although, Al_3Li has a great contribution on strengthening Al-Li alloys, it has been met with only limited success. Therefore, other alloying elements such as Cu and Mg were added to Al-Li alloys to produce more strengthening phases, such as Al_2CuLi, Al_6CuLi_3, and Al_2CuMg.
- The configuration of dislocations is mainly relying upon the size and volume fraction of Al_3Li, where, dislocations move in pairs if fine particles of Al_3Li formed. On the other hand, the dislocations are progressively bowing out between Al_3Li particles with the growth of particles, which lead to decrease the strength of the alloys. The particles which possess a radius less than a critical size may be sheared by the dislocation pairs. However, with the growth of precipitates bowing or bypassing may be occurred.
- The deformation behavior of Al-Li alloys are controlled by several metallurgical factors. These factors include (1) the intrinsic microstructural features (such as the type, size, content, orientation and distribution of strengthening precipitates in both the alloy matrix and grain boundaries and the PFZs at the end of the grain boundaries), and (2) the interactions between these intrinsic microstructural features and dislocation interactions between the dislocations created during the deformation.

Conflict of interest

The authors have declared no conflict of interest.

Compliance with Ethics Requirements

This article does not contain any studies with human or animal subjects.

Acknowledgements

The authors would like to acknowledge the key program supported by the Bureau of international cooperation of the Chinese Academy of Sciences (174321KYSB20150020), the China Postdoctoral Sciences Foundation (2016M590454), Key Research and Development Program of Shenyang (17-32-6-00) and Research Project of State Key Laboratory of Mechanical System and Vibration (MSV201708).

References

[1] Abd El-Aty A, Xu Y, Zhang SH, Ma Y, Chen DY. Experimental investigation of tensile properties and anisotropy of 1420, 8090 and 2060 Al-Li alloys sheet undergoing different strain rates and fibre orientation: a comparative study. Procedia Eng 2017;207:13–8.
[2] Betsofen S, Antipov V, Knyazev M. Al–Cu–Li and Al–Mg–Li alloys: phase composition, texture, and anisotropy of mechanical properties (Review). Russ Metall 2016;2016(4):326–41.
[3] Rioja R, Liu J. The evolution of Al-Li base products for aerospace and space applications. Metall Mater Trans A Phys Metall Mater Sci 2012;43 (9):3325–37.
[4] Lavernia E, Srivatsan T, Mohamed F. Strength, deformation, fracture behaviour and ductility of aluminium-lithium alloys. J Mater Sci 1990;25 (2):1137–58.
[5] Wanhill R, Bray G. Aerostructural design and its application to aluminum-lithium alloys. In: Prasad E, Gokhale A, Wanhill H, editors. Aluminum-lithium alloys: processing, properties, and applications. Butterworth-Heinemann: Elsevier Inc; 2014. p. 28–6.
[6] Prasad N, Gokhale A, Rao P. Mechanical behaviour of aluminium-lithium alloys. Sadhana 2003;28(1–2):209–46.
[7] Giummarra C, Thomas B, Rioja R. New aluminum-lithium alloys for aerospace applications. Proc. Light Met. Technol. Conf.; 2007.
[8] Dursun T, Soutis C. Review: recent developments in advanced aircraft aluminium alloys. Mater Des 2014;56:862–71.
[9] Lavernia E, Grant N. Review: aluminium-lithium alloys. J Mater Sci 1987;22 (5):1521–9.
[10] Alexopoulos N, Migklis E, Stylianos A, Myriounis D. Fatigue behavior of the aeronautical Al–Li 2198 aluminum alloy under constant amplitude loading. Int J Fatigue 2013;56:95–105.
[11] Rao K, Ritchie R. Fatigue of aluminium-lithium alloys. Int Mater Rev 1992;37 (1):153–86.
[12] Magnusen P, Mooy D, Yocum L, Rioja R. Development of high toughness sheet and extruded products for airplane fuselage structures. In: 13th Int. Conf. Alum. Alloy (ICAA13); 2012.
[13] Zakharov V. Some problems of the use of aluminum-lithium alloys. Met Sci Heat Treat 2003;45(1–2):49–54.
[14] Khokhlatova L, Kolobnev N, Oglodkov M, Mikhaylov E. Aluminum-lithium alloys for aircraft building. Metallurgist 2012;56(5–6):336–41.
[15] Kashyap B, Chaturvedi M. Stain anisotropy in AA8090 Al–Li alloy during high temperature deformation. Mater Sci Eng, A 2000;281(1–2):88–95.
[16] Qin H, Zhang H, Wu H. The evolution of precipitation and microstructure in friction stir welded 2195–T8 Al-Li alloy. Mater Sci Eng, A 2015;625:322–9.
[17] Sverdlin A, Drits A, Krimova T, Sergeev K, Ginko I. Aluminium–lithium alloys for aerospace. Adv Mater Process 1998;153(6):49–51.
[18] Adam C, Fish G. Rapidly solidified alloys. Met Forum 1984;7(4):218–32.
[19] Lang L, Liu K, Wu W, Liu B. Optimization research on warm hydroforming process of thin-walled 2060 Al-Li alloy part by FEM simulation. In: 7th Int. Conf. tube hydro (TUBEHYDO 2015); 2015. p. 245–50.
[20] Jin X, Fu B, Zhang C, Liu W. Evolution of the texture and mechanical properties of 2060 alloy during bending. Int J Miner Metall Mater 2015;22(9):966–71.
[21] Jin X, Fu B, Zhang C, Liu W. Strain localization and damage development in 2060 alloy during bending. Int J Miner Metall Mater 2015;22(12):1313–20.
[22] Zhan X, Gu C, Wu H, Liu H, Chen J, Chen J, et al. Experimental and numerical analysis on the strength of 2060 Al–Li alloy adhesively bonded T joints. Int J Adhes Adhes 2016;65:79–87.
[23] Li H, Guo X, Sun Z, Liu H, Wang W, Tao J. Forming performance of a new quenching 2060 aluminum-lithium alloy. In: 6th Int. Conf. tube hydro (TUBEHYDO 2013); 2013. p. 427–34.

[24] Jin X, Fu B, Zhang C, Liu W. Study of dislocation boundary structure in Al–Li alloy during bending. Acta Metall Sin (English Lett) 2015;28(9):1149–55.
[25] Bregianos A, Crosky A, Munroe P, Hellier A. Study aimed at determining and understanding the fracture behaviour of an Al–Li–Cu–Mg–Zr alloy 8090. Int J Fract 2010;161(2):141–59.
[26] Fan W, Kashyap B, Chaturvedi M. Effects of strain rate and test temperature on flow behaviour and microstructural evolution in AA8090 Al–Li alloy. Mater Sci Technol 2001;17(4):431–8.
[27] Chen B, Tian X, Li X, Lu C. Hot deformation behavior and processing maps of 2099 Al-Li alloy. J Mater Eng Perform 2014;23(6):1929–35.
[28] Decreus B, Deschamps A, Donnadieu P, Ehrström J. On the role of microstructure in governing fracture behavior of an aluminum–copper–lithium alloy. Mater Sci Eng, A 2013;586:418–27.
[29] Kumar D, Swaminathan K. Formability of two aluminium alloys. Mater Sci Technol 1999;15(11):1241–52.
[30] Gao H, Weng T, Liu J, Li C, Li Z, Wang L. Hot stamping of an Al-Li alloy: A feasibility study. Manuf Rev 2016;3:9.
[31] Xiang S, Liu D, Zhu R, Li J, Chen Y, Zhang X. Hot deformation behavior and microstructure evolution of 1460 Al−Li alloy. Trans Nonferrous Met Soc China (English Ed.) 2015;25(12):3855–64.
[32] Jagan Reddy G, Srinivasan N, Gokhale A, Kashyap B. Processing map for hot working of spray formed and hot isostatically pressed Al-Li alloy (UL40). J Mater Process Technol 2009;209(18–19):5964–72.
[33] Bate P, Ridley N, Zhang B. Mechanical behaviour and microstructural evolution in superplastic Al–Li–Mg–Cu–Zr AA8090. Acta Mater 2007;55(15):4995–5006.
[34] Denzer D, Rioja R, Bray G, Venema G, Colvin E. The evolution of plate and extruded products with high strength and toughness. In: Weiland H, Rollett AD; 2012. p. 587–92.
[35] Ye L, Zhang X, Zheng D, Liu S, Tang J. Superplastic behavior of an Al–Mg–Li alloy. J Alloy Compd 2009;487(1–2):109–15.
[36] Gao H, Li N, Ho H, Zhang Y, Zhang N, Wang L, et al. Determination of a set of constitutive equations for an Al-Li alloy at SPF conditions. Mater Today: Proc 2015;2:S408–13.
[37] Kaibyshev R, Osipova O. Superplastic behaviour of an Al–Li–Cu–Mg alloy. Mater Sci Technol 2005;21(10):1209–16.
[38] Shagiev M, Motohashi Y, Musin F, Kaibyshev R, Itoh G. Superplastic Behavior in Al–Li–Mg–Cu–Sc Alloy Sheet. Mater Trans 2003;44(9):1694–7.
[39] Adamczyk-Cie-slak B, Mizera J, Kurzydłowski KJ. Thermal stability of model Al-Li alloys after severe plastic deformation-effect of the solute Li atoms. Mater Sci Eng, A 2010;527(18–19):4716–22.
[40] Bae D, Ghosh A. Cavity growth in a superplastic Al-Mg alloy. II. An improved plasticity based model. Acta Mater 2002;50(5):1011–29.
[41] Bae D, Ghosh A. Cavity formation and early growth in a superplastic Al-Mg alloy. Acta Mater 2002;50(3):511–23.
[42] Bae D, Ghosh A. Cavity growth during superplastic flow in an Al-Mg alloy. I. Experimental study. Acta Mater 2002;50(5):993–1009.
[43] Es-Said O, Parrish C, Bradberry C, Hassoun J, Parish R, Nash A, et al. Effect of stretch orientation and rolling orientation on the mechanical properties of 2195 Al-Cu-Li alloy. J Mater Eng Perform 2011;20(7):1171–9.
[44] Giuliano G. Constitutive equation for superplastic Ti-6Al-4V alloy. Mater Des 2008;29(7):1330–3.
[45] Ou L, Zheng Z, Nie Y, Jian H. Hot deformation behavior of 2060 alloy. J Alloy Compd 2015;648:681–9.
[46] Xiaoxin X, Martin J. High-temperature deformation of AI-Li-Cu-Mg-Zr alloys 8090 and 8091. J Mater Sci 1992;27(3):592–8.
[47] Haghshenas M, Khalili A, Ranganathan N. On room-temperature nanoindentation response of an Al-Li-Cu alloy. Mater Sci Eng, A 2016;676:20–7.
[48] Li X, Song N, Guo G, Sun Z. Prediction of forming limit curve (FLC) for Al–Li alloy 2198–T3 sheet using different yield functions. Chinese J Aeronaut 2013;26(5):1317–23.
[49] Xu Y, Zhong W, Chen Y, Shen L, Liu Q, Bai Y, et al. Shear localization and recrystallization in dynamic deformation of 8090 Al–Li alloy. Mater Sci Eng, A 2001;299(1–2):287–95.
[50] Gupta R, Nayan N, Nagasireesha G, Sharma S. Development and characterization of Al-Li alloys. Mater Sci Eng, A 2006;420(1–2):228–34.
[51] Baron I. US Patent 2,381,219, 1945-08-07.
[52] Criner C. Aluminum base alloy, U.S. Patent No. 2,784,126, Issued March 5, 1957.
[53] Criner C. Aluminum Base Alloy, U.S. Patent No. 2,915,391, Issued December 11959.
[54] Starke E, Staley J. Application of modern aluminum alloys to aircraft. Prog Aerosp Sci 1996;32(2–3):131–72.
[55] Starke E, Lin F. The influence of grain structure on the ductility of the Al–Cu–Li–Mn–Cd alloy 2020. Metall Trans A 1982;13:2259–69.
[56] Sampath D, Dashwood R, McShane H, Sheppard T. Microstructure and property development in low density rapidly solidified Al-Li alloys. Mater Sci Technol 1993;9(3):218–27.
[57] Starke E. Review of the development, microstructure and properties of new al-li alloys. Congr Int Counc Aeronaut Sci 1986;2:934–43.
[58] Starke E, Sanders T, Palmer I. New approaches to alloy development in the Al–Li system. J Miner Met Mater Soc 1981;33(8):24–33.
[59] Starke E. Historical development and present status of aluminum-lithium alloys. In: Prasad E, Gokhale A, Wanhill H, editors. Aluminum-lithium alloys: processing, properties, and applications. Butterworth-Heinemann: Elsevier Inc; 2014. p. 3–26.
[60] Miller W, Zhuang L, Bottema J, Wittebrood A, De Smet P, Haszler A, et al. Recent development in aluminium alloys for the automotive industry. Mater Sci Eng, A 2000;280(1):37–49.
[61] Meyer P, Dubost B. Production of Al-Li alloy with high specific properties. Aluminum Lithium Alloys III, the Institute of Metals, London, U.K.; 1986. p. 37–46.
[62] Rioja R. Fabrication methods to manufacture isotropic Al-Li alloys and products for space and aerospace applications. Mater Sci Eng, A 1998;257(1):100–7.
[63] Fridiyander N, Bratukhin G, Davydov G. Soviet Al-Li alloys of aerospace applications. In: Peters M, Jinkler P, editors. DGM Information sgesellschaft mbH, Germany; 1992. P. 35–42.
[64] Staley J, Lege D. Advances in aluminium alloy products for structural applications in transportation. Le J Phys IV 1993; 03(C7): C7–179-C7-190.
[65] Bodily B, Heinimann M, Bray G, Colvin E, Witters J. Advanced aluminum and aluminum–lithium solutions for derivative and next generation aerospace structures. SAE paper no 2012-01-1874.
[66] Srivatsan T, Lavernia E, Eswara Prasad N, Kutumbarao V. Quasi-static strength, deformation, and fracture behavior of aluminum-lithium alloys. In: Prasad E, Gokhale A, Wanhill H, editors. Aluminum-lithium alloys: processing, properties, and applications. Butterworth-Heinemann: Elsevier Inc; 2014. p. 305–39.
[67] Ashton RF, Thompson DS, Gayle FW. The effect of processing on the properties of Al_Li alloys. In: Starke J, Sanders J, editors. Aluminum alloys-their physical and mechanical properties. EMAS, Warley, England; 1986. p. 403–17.
[68] Prasad K, Prasad N, Gokhale A. Microstructure and precipitate characteristics of aluminum-lithium alloys. In: Prasad E, Gokhale A, Wanhill H, editors. Aluminum-lithium alloys: processing, properties, and applications. Butterworth-Heinemann: Elsevier Inc; 2014. p. 99–37.
[69] Narayanan G, Quist W, Wilson B, Wingert A. Low density aluminium alloy development. First Interim Technical Report, AFWAL Contract No. F33615–81-C- 5053, Air Force Wright Aeronautical Laboratories, Dayton, Ohio, USA; 1982.
[70] Furukawa M, Miura Y, Nemoto M. Strengthening mechanisms in Al-Li alloys containing coherent ordered particles. Trans Jpn Inst Met 1985;26(4):230–5.
[71] Furukawa M, Miura Y, Nemoto M. Arrangement of deformation induced dislocations in aged Al-Li alloys. Trans Jpn Inst Met 1985;26(4):225–9.
[72] Csontos A, Starke E. The effect of processing and microstructure development on the slip and fracture behavior of the 2.1 wt pct Li AF/C-489 and 1.8 wt pct Li AF/C-458 Al-Li-Cu-X alloys. Metall Trans A 2000;31(8):1965–76.
[73] Noble B, Harris S, Dinsdale K. The elastic modulus of aluminium-lithium alloys. J Mater Sci 1981;17(2):461–8.
[74] Noble B, Harris S, Dinsdale K. Yield characteristics of aluminium-lithium alloys. Met Sci 1982;16(9):425–30.
[75] Lin F, Chakraborty S, Starke E. Microstructure-property relationships of two Al-3Li-2Cu-0.2Zr-X Cd alloys. Metall Trans A 1982;13(3):401–10.
[76] Suresh S, Vasudevan A, Tosten M, Howell P. Microscopic and macroscopic aspects of fracture in lithium containing aluminium alloys. Acta Metall 1987;35(1):25–46.
[77] Cassada W, Shiflet G, Starke E. Grain boundary precipitates with five-fold diffraction symmetry in an Al-Li-Cu alloy. Scr Metall 1986;20(5):751–6.
[78] Webster D. Aluminum-lithium powder metallurgy alloys with improved toughness. Metall Trans A 1988;19(3):603–15.
[79] Webster D. The effect of low melting point impurities on the properties of aluminum-lithium alloys. Metall Trans A 1987;18(12):2181–93.
[80] Hill D, Williams D, Mobley C. The effect of hydrogen on the ductility, toughness and yield strength of an Al-Mg-Li alloy. In: Sanders T, Starke E, editors. Proc. 2nd int. conf. aluminum-lithium alloy. The metallurgical society of AIME. Warrendale, PA; 1984. p. 201–218.
[81] Srivatsan T, Place T. Microstructure, tensile properties and fracture behaviour of an Al-Cu-Li-Mg-Zr alloy 8090. J Mater Sci 1989;24(5):1543–51.
[82] Srivatsan T, Lavernia E. The presence and consequences of precipitate free zones in an aluminium-copper-lithium alloy. J Mater Sci 1991;26(4):940–50.
[83] Jata K, Starke E. Fatigue crack growth and fracture toughness behaviour of an Al-Li-Cu alloy. Metall Trans A 1986;17(6):1011–26.
[84] Srivatsan T, Yamaguchi K, Starke E. The effect of environment and temperature on the low cycle fatigue behavior of aluminum alloy 2020. Mater Sci Eng 1986;83(1):87–107.
[85] Peel C, McDarmaid D, Evans B. Considerations of critical factors for the design of aerospace structures using current and future Al-Li alloys. In: Park M, Kar R, Agarwal S, Quist W, editors. Aluminium_lithium alloys: design, development and applications update. OH: ASM International; 1988. p. 315–37.
[86] Gregson P, Flower H, Tete C, Mukhopadhyay A. Role of vacancies in precipitation of δ0- and S-phases in Al-Li-Cu-Mg alloys. Mater Sci Technol 1986;2(4):349–53.
[87] Flower H, Gregson P. Solid state phase transformations in aluminium alloys containing lithium. Mater Sci Technol 1987;3(2):81–90.
[88] Dinsdale K, Harris SJ, Noble B. Relationship between microstructure and mechanical properties of aluminium-lithium-magnesium alloys. In: Sanders T, Starke E, editors. Proc. 1st int. conf. aluminum-lithium alloy. The metallurgical society of AIME. Warrendale, PA; 1981. p. 101–18.

[89] Mukhopadhyay A, Flower H, Sheppard T. Development of microstructure in AA 8090 alloy produced by extrusion processing. Mater Sci Technol 1990;6(5):461–8.
[90] Roters F, Eisenlohr P, Hantcherli L, Tjahjanto D, Bieler T, Raabe D. Overview of constitutive laws, kinematics, homogenization and multiscale methods in crystal plasticity finite-element modeling: Theory, experiments, applications. Acta Mater 2010;58(4):1152–211.
[91] Piehler H. Crystal-plasticity fundamentals. In: Fundamentals of modelling for metals processing, ASM Handbook; 2009; 22(2): p. 232-238.
[92] Eswara Prasad N, Malakondaiah G, Kutumbarao V, Rama Rao P. In-plane anisotropy in low cycle fatigue properties of and bilinearity in Coffin-Manson plots for quaternary Al-Li-Cu-Mg 8090 alloy plate. Mater Sci Technol 1996;12(7):563–77.
[93] Pasang T, Symonds N, Moutsos S, Wanhill R, Lynch S. Low-energy intergranular fracture in Al-Li alloys. Eng Fail Anal 2012;22:166–78.
[94] Jata KV, Singh AK. Texture and its effects on properties in aluminum-lithium alloys. In: Prasad E, Gokhale A, Wanhill H, editors. Aluminum-lithium alloys: processing, properties, and applications. Butterworth-Heinemann: Elsevier Inc; 2014. p. 139–63.
[95] Kim S, Huh H, Bok H, Moon M. Forming limit diagram of auto-body steel sheets for high-speed sheet metal forming. J Mater Process Technol 2001;211(5):851–62.
[96] Kalyanam S, Beaudoin A, Dodds R, Barlat F. Delamination cracking in advanced aluminium–lithium alloys-experimental and computational studies. Eng Fract Mech 2009;76(14):2174–91.
[97] Pasang T, Lynch S, Moutsos S. Challenges in developing high performance Al-Li alloys. Int J Soc Mater Eng Resour 2006;14(1–2):7–11.
[98] Vasudevan A, Fricke W, Malcolm R, Bucci R, Przystupa M, Barlat F. On through thickness crystallographic texture gradient in Al-Li-Cu-Zr alloy. Metall Trans A 1988;19(3):731–2.
[99] Smith S, Scully J. The identification of hydrogen trapping states in an Al-Li-Cu-Zr alloy using thermal desorption spectroscopy. Metall Mater Trans A 2000;31(1):179–93.
[100] Jata K, Singh A. Texture and its effects on properties in aluminum-lithium alloys. In: Prasad E, Gokhale A, Wanhill H, editors. Aluminum-lithium alloys: processing, properties, and applications. Butterworth-Heinemann: Elsevier Inc; 2014. p. 140–60.
[101] Vasudevan A, Przystupa M, Fricke W. Texture-microstructure effects in yield strength anisotropy of 2090 sheet alloy. Scr Metall Mater 1990;24(8). 1429-1234.
[102] Vasudevan A, Przystupa M, Fricke W. Effect of composition on crystallographic texture of hot rolled Al-Li binary alloys. Mater Sci Eng, A 1995;196(1–2):1–8.
[103] Choi S, Barlat F. Prediction of macroscopic anisotropy in rolled aluminum-lithium sheet. Scr Mater 1999;41(9):981–7.
[104] Barlat F, Liu J. Precipitation induced anisotropy in binary Al-Cu alloys. Mater Sci Eng, A 1998;257(1):47–61.
[105] Barlat F, Bren J, Liu J. On crystallographic texture gradient and its mechanical consequence in rolled aluminum-lithium sheet. Scr Metall Mater 1992;27(9):1121–6.
[106] Garmestani H, Kaldindi S, Williams L, Bacaltchuk C, Fountain C, Lee E, et al. Modelling the evolution of anisotropy in Al-Li alloys: application to Al-Li 2090–T8E41. Int J Plast 2002;18(10):1373–93.
[107] Hargarter H, Lyttle M, Starke E. Effect of preferentially aligned precipitates on plastic anisotropy in Al-Cu-Mg-Ag and Al-Cu alloys. Mater Sci Eng, A 1998;257(1):87–99.
[108] Lyttle M, Wert J. The plastic anisotropy of an Al-Li-Cu-Zr alloy extrusion in unidirectional deformation. Metall Mater Trans A 1996;27(11):3503–13.
[109] Fox S, Flower H. McDarmaid D. Formation of solute-depleted surfaces in Al-Li-Cu-Mg-Zr alloys and their influence on mechanical properties. In: Baker C, Gregson P, Harris S, Peel C, editors. Proc. 3rd Int. Conf. Aluminum-Lithium Alloy, vol. 3. The Institute of Metals, London; 1986. p. 263–72.
[110] Starke E. Aluminum alloys of the 70's: scientific solutions to engineering problems. Mater Sci Eng 1977;29(2):99–115.
[111] Tempus G, Calles W, Scharf G. Influence of extrusion process parameters and texture on mechanical properties of Al-Li extrusions. Mater Sci Technol 1991;7(10):937–45.
[112] Takahashi K, Minakawa K, Ouchi C. The effect of thermomechanical processing variables on anisotropy in mechanical properties of Al-Li alloys. In: Champier G, Dubost B, Miannay D, Sabetay L, editors. Proc. 3rd int. conf. aluminum-lithium alloy. J. Phys. Colloques; 1987 48(C3). p. 163–69.
[113] Bodily B, Heinimann M, Bray G, Colvin E, Witters J. Advanced aluminum and aluminum–lithium solutions for derivative and next generation aerospace structures. SAE 2012. doi: https://doi.org/10.4271/2012-01-1874.
[114] Engler O, Lücke K. Influence of the precipitation state on the cold rolling texture in 8090 Al-Li material. Mater Sci Eng, A 1991;148(1):15–23.
[115] Yuan Z, Lu Z, Xie Y, Wu X, Dai S, Liu C. Mechanical properties of a novel high strength aluminium–lithium alloy. Mater Sci Forum 2011;689:385–9.
[116] Bron F, Besson J. A yield function for anisotropic materials: Application to aluminium alloys. Int J Plast 2004;20(4–5):937–63.
[117] Chen J, Mady Y, Morgeneyer F, Besson J. Plastic flow and ductile rupture of a 2198 Al-Cu-Li aluminium alloy. Comput Mater Sci 2011;50(4):1365–71.
[118] Dorward R. Zirconium vs manganese-chromium for grain structure control in an Al-Cu-Li alloy. Metall Trans 1987;18(10):1820–3.
[119] Lee E, Kalu P, Brandao L, Es-Said O, Foyos J, Garmestani H. The effect of off-axis thermo mechanical processing on the mechanical behavior of textured 2095 Al-Li alloy. Mater Sci Eng, A 1999;265(1–2):100–9.
[120] Cho C, Sawtell R. Al-Li alloys and method of making the same, U.S. Patent No. 5, 066, 342, 1991. p. 11–19.
[121] Jata K, Hopkins A, Rioja R. The Anisotropy and Texture of Al-Li Alloys. Mater Sci Forum 1996;217–222:647–52.

Ali Abd El-Aty is a PhD student at advanced metal forming technology group (AMFT), Institute of metal research (IMR), Chinese academy of sciences (CAS), Shenyang, China from October 2015 to-date. Besides, he is an assistant lecturer at mechanical engineering department, faculty of engineering, Helwan University, Cairo, Egypt from June 2013 to-date. Mr. Ali has been graduated from mechanical engineering department, Helwan University, Egypt in 2007 and worked as a teaching assistant at the same department from June 2009 to June 2013. In June 2013, he received master of science (M. SC.) in the field of Mechanical Engineering from the same university. From Sept. 2013 to Sept. 2014 he was a visiting student at advanced materials and mechanics lab, mechanical engineering Department, Pohang University of Science and Technology (POSTECH), Pohang, Republic of Korea. The research and industrial experiences of Mr. Ali are on a range of sheet metal forming processes, such as sheet and tube hydroforming, stamping as well as superplastic forming. His research interests include materials modelling and characterization, Formulation and determination of constitutive equations, Crystal plasticity finite element modelling (CPFEM), and Formability prediction and enhancement. Currently, He is investigating the deformation behavior and anisotropic response of Al-Li alloys sheets such as AA1420, AA8090, AA2198-T851, AA2050 and AA2060-T8 over wide range of temperatures and strain rates using experimentation and finite element modelling.

Yong Xu is an associate professor at Institute of Metal Research (IMR), Chinese Academy of Sciences (CAS), and a main member of advanced metal forming technology group (AMFT). In 2012, he was received his doctoral degree in the field of Materials Sciences and Engineering from Institute of Metal Research (IMR), Chinese Academy of Sciences (CAS). In his PhD study, Prof. Xu successfully revealed the mechanism of formability improvement of austenitic stainless steel by pulsating load. The research interests of Prof. Xu include the development of advanced flexible forming technologies and machines for complex shaped thin-walled components, microstructure evolution and mechanical properties of high-performance alloys, finite element simulation and multi-scale modelling. He is currently working on developing novel sheet/tube hydroforming technology such as pulsating hydroforming, impact hydroforming and hydro-forging to improve the formability of advanced structure materials such as high strength steel, stainless steel, Mg alloy, Al alloy and Al-Li Alloy; Multi-scale mechanics of materials; Predicting of texture evolution and anisotropic behavior by CPFEM; Sheet metal formability (prediction and improvement). His research works were funded by National Natural Science Foundation of China and China Postdoctoral Sciences Foundation and the main achievements have been successfully applied in Chinese automobile, aviation and nuclearpower industry. To-date, Prof. Xu has published more than 30 journal papers published in international and Chinese leading SCI and EI journals and got around 20 patents.

Xunzhong Guo is an associate professor at Advanced forming research institute, College of Material Science and Technology, Nanjing University of Aeronautics and Astronautics, Nanjing, China. The research interests of Prof. Guo are precision hydroforming of tubular and thin-walled parts, preparation and secondary plastic forming of the laminate materials, FE simulation of plastic forming processes and Multi-scale mechanics of Materials. Prof. Guo has published more than 37 papers, additionally, his papers have been cited over 112 times from the SCI papers in the past five years.

Prof. Shi-Hong Zhang is a leader of advanced metal forming technology group and vice director of Specialized Materials and Devises Division Shenyang R & D Centre for Advanced Materials, Institute of Metal Research (IMR), Chinese Academy of Sciences (CAS), China. Additionally, he is a director of Engineering Research Centre for Precision Copper Tubes (ERC/PCT), Chinese Academy of Sciences as well as he is Vice President of Chinese Society for Technology of Plasticity (CSTP, in charge of international cooperation). Prof. Zhang received his B.Sc., M.Sc. and PhD from Department of Mechanics, Harbin Institute of Technology (HIT), Harbin, China in 1985, 1988 and 1991 respectively. In 1993, Prof. Zhang was appointed as Associate Professor at HIT till 1995. The same year, he joined DANFOSS A/S, Denmark as a researcher till 1996. Afterwards, he joined Department of Production Engineering, Aalborg University, Denmark as a researcher till 1998. The same year, Prof Zhang was appointed as a Full Professor at School of Materials Sciences and Engineering, HIT, China. From 1999 to-date Prof. Zhang is a full professor at Institute of Metal Research, Chinese Academy of Sciences (IMR/ CAS) in China and the leader of Advanced Metal Forming Technology Group (AMFT), IMR/ CAS. Prof. Zhang has published more than 250 journal papers (around 100 and 150 articles published in international and Chinese leading SCI journals respectively), 56 conference papers and got around 50 patents. His papers have been cited over 1500 times from the SCI papers and also cited over 2000 times from the papers published in China in the past five years. The research interests of Prof. Zhang include Development of Advanced Metal forming Technologies (Impact hydroforming, Pulsating hydroforming, stamping, rolling, cross wedge rolling, pilgering, and stretch forming processes); Finite Element Modelling of Metal Forming processes; Materials Modelling & characterization; Microstructure evolution and analysis; Predicting of rolling texture by VPSC and CPFEM; Formulation and determination of Constitutive Equations; Multi-Scale Mechanics of Materials; Sheet Metal Formability (prediction and improvement); Modelling of Anisotropic behaviour of Mg. and Al. alloys; Modelling of Strain Path change effect; Cold/Warm deformation of Mg. and Al. alloys; High strain rate deformation and fracture Mechanics.

Yan Ma is a PhD student at advanced metal forming technology group (AMFT), Institute of metal research (IMR), Chinese academy of sciences (CAS) from September 2014 to-date. He has been graduated from Material Science and Engineering School, Shenyang Aerospace University, Shenyang, China in 2007 and he was worked as a lecturer at Liaoyang vocational college of technology from June 2007 to July 2014. In April 2012, he received his master degree in the field of Software Engineering from Software College of Jilin University, China. From Sept. 2014 to-date, he was a cooperative training staff of IMR, CAS mainly worked on the project of hydroforming. His research and industrial experiences are on a range of metal forming processes, such as sheet and tube hydroforming, tube drawing as well as cross wedge rolling. His research interests include Finite Element modelling, development and design of plastic forming processes and optimization of FEM and experiment. Recently, He is investigating the dynamic behavior and formability of Al and Al-Li alloys under high strain rate deformation based on impact hydroforming.

Dayong Chen is a PhD student at advanced metal forming technology group (AMFT), Institute of metal research (IMR), Chinese academy of sciences (CAS) from September 2015 to-date. He has been graduated from Material Science and Engineering School, Shenyang Ligong University, Shenyang, China in 2010 and worked as a junior technician at Echom from June 2010 to July 2011. In April 2015, he received his master degree in the field of Material Processing Engineering from Material Science and Engineering School, Shenyang Ligong University, China. From Sept. 2012 to Apr. 2015 he was a cooperative training staff of IMR, CAS mainly worked on the project of process control of drawing with the floating plug on TP2 tube. His research and industrial experiences are on a range of metal forming processes, such as sheet and tube hydroforming, tube drawing as well as cross wedge rolling. His research interests include Finite Element modelling, development and design of plastic forming processes and optimization of FEM and experiment. Currently, He is investigating the deformation mechanisms, Fracture behavior and formability of the Al alloys based on impact hydroforming.